Title: Distinct roles of cellular ESCRT-I and ESCRT-III proteins in efficient entry and egress of budded virions of Autographa californica multiple nucleopolyhedrovirus

Qi Yue[1+], Qianlong Yu[1+], Qi Yang[1], Ye Xu[1], Ya Guo[1], Gary W. Blissard[2], Zhaofei Li*[1]

[1]State Key Laboratory of Crop Stress Biology for Arid Areas, Key Laboratory of Northwest Loess Plateau Crop Pest Management of Ministry of Agriculture, College of Plant Protection, Northwest A&F University, Yangling, Shaanxi 712100, China

[2]Boyce Thompson Institute, Cornell University, Ithaca, New York 14853

[+]These authors contributed equally to the work

Running Title: Requirement for the ESCRT system in AcMNPV infection

Keywords: ESCRT-I, ESCRT-III, baculovirus, AcMNPV, virus entry and egress

Word count: Abstract, 249 words; Text, 12597 words.

*Corresponding author
Zhaofei Li
College of Plant Protection, Northwest A&F University,
No.3 Taicheng Road, Yangling, Shaanxi, China, 712100
E-mail: zhaofeili73@outlook.com
Tel: 86-18792598371

Abstract

The endosomal sorting complex required for transport (ESCRT) machinery is necessary for budding by many enveloped viruses. Recently, it was demonstrated that Vps4, the key regulator for recycling of the ESCRT-III complex, is required for efficient infection of the baculovirus, *Autographa californica multiple nucleopolyhedrovirus* (AcMNPV). However, ESCRT assembly, regulation and function are complex and little is known regarding details of participation of specific ESCRT complexes in AcMNPV infection. In this study, the core components of ESCRT-I (Tsg101 and Vps28) and ESCRT-III (Vps2B, Vps20, Vps24, Snf7, Vps46, and Vps60) were cloned from *Spodoptera frugiperda*. Using a viral complementation system and RNAi assays, we found that ESCRT-I and ESCRT-III complexes are required for efficient entry of AcMNPV into insect cells. In cells knocking down or overexpressing dominant-negative (DN) forms of the components of ESCRT-I and ESCRT-III complexes, entering virions were partially trapped within the cytosol. To examine only egress, cells were transfected with the dsRNA targeting an individual ESCRT-I or ESCRT-III gene and viral bacmid DNA or viral bacmid DNA that expressed DN forms of ESCRT-I and ESCRT-III components. We found that ESCRT-III components (but not ESCRT-I components) are required for efficient nuclear egress of progeny nucleocapsids. In addition, we found that several baculovirus core or conserved proteins (Ac11, Ac76, Ac78, GP41, Ac93, Ac103, Ac142, and Ac146) interact with Vps4 and components of ESCRT-III. We propose that these viral proteins may form an “egress complex” that is involved in recruiting ESCRT-III components to a virus egress domain on the nuclear membrane.

Importance

The ESCRT system is hijacked by many enveloped viruses, to mediate budding and release. Recently, it was found that Vps4, the key regulator of cellular ESCRT machinery, is necessary for efficient entry and egress of *Autographa californica multiple nucleopolyhedrovirus* (AcMNPV). However, little is known about the roles of specific ESCRT complexes in AcMNPV infection. In this study, we demonstrated that ESCRT-I and ESCRT-III complexes are required for efficient entry of AcMNPV into insect cells. The components of ESCRT-III (but not ESCRT-I) are also necessary for efficient nuclear egress of progeny nucleocapsids. Several baculovirus core or conserved proteins were found to interact with Vps4 and components of ESCRT-III, and these interactions may suggest the formation of an “egress complex” involved in nuclear release or transport of viral nucleocapsids.

Introduction

The endosomal sorting complex required for transport (ESCRT) comprises five distinct protein complexes denoted as ESCRT-0, I, II, III, and the AAA ATPase, Vps4, plus some ESCRT-associated proteins, such as Alix (1, 2). ESCRT-0 is required for selectively sorting ubiquitinated membrane proteins and recruiting ESCRT-I. ESCRT-I, a heterotetramer complex composed of Vps23 (Tsg101), Vps28, Vps37, and MVB12/UBP1, in turn recruits the heterotetramer ESCRT-II complex. ESCRT-II is comprised of Vps22, Vps36, and two molecules of Vps25. ESCRT-I/-II interact with ubiquitinated cargo proteins and membrane phospholipids and this larger complex is involved in generating membrane curvature and creating membrane buds. Within the membrane bud neck, ESCRT-I/-II and Alix recruit ESCRT-III and promote formation of ESCRT-III polymers that result in filament or ring formation. It is believed that constriction of this ring results in scission of the newly budded vesicle (3, 4). ESCRT-III is a dynamic polymer complex and its components are conserved from Archaea to mammalians. In yeast and humans, ESCRT-III contains a set of closely-related proteins, including Vps2 [two isoforms in humans termed charged multivesicular body protein 2A and 2B (CHMP2A and CHMP2B)], Vps20 (CHMP6), Vps24 (CHMP3), Vps32/Snf7 (CHMP4A, CHMP4B, CHMP4C), Vps46 (CHMP1A, CHMP1B), Vps60 (CHMP5), and IST1. Among these components, Vps2, Vps20, Vps24, and Snf7 serve as the “core” proteins to build the ESCRT-III helical filaments (5). Following ESCRT-III mediated membrane scission, the ESCRT-III complex is disassembled by Vps4 in an ATP-dependent manner (1, 4, 6, 7). The activity of Vps4 is regulated by its cofactor Vta1 (8). Initially, the ESCRT system was identified as an essential membrane remodeling and scission machinery for sorting

ubiquitinated membrane proteins into intraluminal vesicles of multivesicular bodies (MVBs)(9). Components of the ESCRT pathway are also involved in a variety of other biological processes, including the abscission stage of cytokinesis, biogenesis of exosomes, plasma membrane wound repair, neuron pruning, extraction of defective nuclear pore complexes, nuclear envelope reformation, and budding of virus particles (2, 10-13).

It was previously discovered that many enveloped viruses hijack components of the ESCRT pathway to mediate virus budding and release from infected cells (12). The detailed mechanism of ESCRT-mediated virus budding has been examined extensively in retroviruses, particularly HIV-1. Retroviral Gag proteins contain late assembly domains (L-domains) with consensus sequences such as PPXY, P(T/S)AP, YPXnL. These L-domains mediate interactions of Gag with cellular proteins such as NEDD4-like ubiquitin ligases, ESCRT-I component Tsg101, and Alix. Through specific protein-protein interactions, Gag proteins bind and recruit ESCRT-I and/or Alix, which in turn recruit and direct localization of ESCRT-III and Vps4 to regions of the plasma membrane where virion budding occurs (12, 14-16). Involvement of the ESCRT pathway in non-enveloped virus release was also observed for Bluetongue virus and Hepatitis A (17, 18). In addition to their importance in viral egress, components of the ESCRT system were also found to be required for the entry of some enveloped viruses, including Kaposi's sarcoma-associated herpesvirus (KSHV), Crimean-Congo hemorrhagic fever virus (CCHFV), vesicular stomatitis virus (VSV), *Autographa californica multiple nucleopolyhedrovirus* (AcMNPV), and the non-enveloped rhesus rotavirus (RRV) (19-23). Most recently,

ESCRT-I/-III have been shown to function in formation of a viral replication compartment during infection by certain positive-strand RNA viruses of plants (24).

AcMNPV is the most intensively studied baculovirus and is the type species of the virus family *Baculoviridae* (25). Baculoviruses are enveloped, insect-specific double-stranded DNA viruses that replicate in the nuclei of infected cells. During the infection cycle, baculoviruses produce two phenotypes of enveloped virions: occlusion-derived virions (ODV) and budded virions (BV). ODV and BV appear to share identical nucleocapsids and genome content, but differ in the source and composition of their envelopes and in their roles in virus infection (25). ODV initiate infection of insect midgut epithelial cells upon oral ingestion of occlusion bodies (OBs) and are responsible for spreading viral infection horizontally among insects. The nucleocapsids of ODV are enveloped in the nucleus by membranes derived from intranuclear microvesicles, which are derived from the inner nuclear membrane (26, 27). The BV transmit infection from cell-to-cell within and between insect tissues, and BV are highly infectious in cultured cell lines. The envelopes of BV are acquired from the plasma membrane during virion budding and release (25). Budded virions of AcMNPV enter cells via clathrin-mediated endocytosis (28). During the entry process by BV, the major viral envelope glycoprotein GP64 mediates receptor binding and low-pH triggered membrane fusion (29, 30). After release into the cytoplasm, nucleocapsids nucleate the formation of actin filaments as a propulsion mechanism, and are eventually delivered into the nucleus through nuclear pores (31, 32). In the nucleus, viral early gene transcription is followed by DNA replication and late gene transcription. At a relatively early stage of infection, progeny nucleocapsids are transported from the nucleus to the plasma membrane by a

125 mechanism that is largely unknown. Then, the nucleocapsids bud and are pinched off
126 from the plasma membrane to form BV (25). The cell surface localized GP64 is also
127 important for virion budding (33). At a late stage of infection, most of the assembled
128 nucleocapsids appear to be retained within the nucleus to form virions of the ODV
129 phenotype (25). In recent years, numerous gene knockout studies have reported that
130 certain baculovirus core genes (such as Ac76, Ac78, Ac93, Ac103, Ac142, and Ac146)
131 are required for production of infectious AcMNPV BV. However, it is not clear how these
132 viral proteins are involved in virus infection (34-39).

133 Recently, we found that the ESCRT pathway is conserved in sequenced insect
134 genomes and that the expression levels of certain components of ESCRT-I, II, III, Vps4,
135 and Alix were significantly up-regulated upon AcMNPV infection (40, 41). In addition,
136 prior studies revealed that efficient entry and egress of AcMNPV BV are dependent on
137 functional Vps4 (23). Since Vps4 is required for recycling of ESCRT III and represents a
138 terminal step in the ESCRT pathway, this suggests that other components of the ESCRT
139 pathway may be specifically involved in entry and egress. To investigate the potential
140 roles of other ESCRT components in efficient production of infectious BV of AcMNPV,
141 we cloned ESCRT-I [Vps23 (Tsg101) and Vps28] and ESCRT-III (Vps2B, Vps20, Vps24,
142 Vps32/Snf7, Vps46, and Vps60) cDNAs, then knockdown or generated and expressed
143 dominant-negative forms of these proteins in insect cells. We found that ESCRT-I and
144 ESCRT-III were both required for efficient entry of AcMNPV, whereas ESCRT-III was
145 also involved in egress of AcMNPV BV. We also identified interactions of certain ESCRT
146 pathway proteins with viral core proteins that are required for infectious BV production.

147 We propose that these viral proteins form a complex to recruit ESCRT-III/Vps4 to virion
148 budding and releasing regions at the nuclear membrane.

Journal of Virology

149 ## Materials and Methods

150 ### Cells, transfections, and infections

151 *Spodoptera frugiperda* (Sf9) and *Trichoplusia ni* (High 5), and $Sf9^{Op1D}$ (a cell line
152 expressing the *Orgyia pseudotsµgata* (Op)MNPV GP64 protein) cells (42) were cultured
153 at 27° in TNMFH medium (Sigma-Aldrich) containing 10% fetal bovine serum (FBS,
154 Gibco). Transfection of plasmid DNAs or double-strand (ds)RNA in 12-well plate ($2X10^5$
155 cells per well) was performed using a standard $CaPO_4$ precipitation procedure (29), and
156 viral bacmid transfections in 6-well plate ($1X10^6$ cells/well) using Cellfectin II reagent
157 (Invitrogen). For viral infections, the virus was incubated on cells for 1 h, and then cells
158 were washed once in TNMFH. Times post infection (p.i.) were calculated from the time
159 the viral inoculum was added.

160 ### Cloning and mutagenesis of ESCRT-I and ESCRT-III components

161 Total RNA was isolated from Sf9 cells by using Trizol reagent RNAiso plus
162 (TaKaRa), and the first strand cDNA synthesis was performed with AMV reverse
163 transcriptase using RNA LA PCR kit (TaKaRa). Gene-specific primers (Table 1) targeted
164 to the outside regions of the open reading frame (ORF) of ESCRT-I components Tsg101
165 and Vps28, and ESCRT-III components Vps2B, Vps20, Snf7, Vps46, and Vps60 were
166 designed based on the EST sequences at SPODOBASE database
167 (http://bioweb.ensam.inra.fr/spodobase/) (43), and used to amplify the complete ORF
168 and partial 5' and 3' ends of each gene, from the cDNA. Another set of gene-specific
169 primers were further designed and used to PCR amplify the complete ORF of the above
170 ESCRT components. To obtain the ESCRT-III component Vps24, 3' RACE (rapid
171 amplification of cDNA ends) was conducted with 3'-Full RACE Core Set with

PrimeScript™ RTase (TaKaRa) and gene-specific primers Vps24SP1 and Vps24SP2 (Table 1). Two primers specific for 5' and 3' ends of Vps24 and two primers specific for the ORF of Vps24 were further designed according to SPODOBASE database and 3'RACE sequences, and used to PCR amplify the ORF of Vps24.

To remove the XbaI site within the ORF of Snf7 for subsequent cloning, a silent mutation was introduced by over-lap PCR using the pair primers Snf7XF and Snf7mR, and Snf7mF and Snf7ER (Table 1). The truncated forms of Tsg101 and Vps28 were generated by PCR. All the PCR products were cloned into pMD18-T vector (TaKaRa) and sequenced with M13-47 and M13-48 primers. The pMD18-T vector containing the ORF or the truncated forms of ESCRT-I and ESCRT-III components was designated as X-pMD18-T or Y-pMD18-T (X, Y represents ESCRT-I and ESCRT-III components, respectively).

Construction of plasmids, bacmids, and viruses

All expression plasmids were listed in Table 2. Initially, to generate the transient expression vector pIEnGFP and pIEcGFP, the ORF of enhanced green fluorescent protein (EGFP) and a fragment containing the ORF of EGFP and the poly(A) signal of the AcMNPV *gp64* gene were amplified by PCR using Vps4-gfppBlue (23) as template and separately inserted between XbaI and BamHI, or EcoRI and HindIII sites of the plasmid pIE (44). For generating ESCRT-I components Tsg101- and Vps28- derived expression plasmids, the ORF and truncated forms of Tsg101 and Vps28 were isolated from X-pMD18-T with enzymes BamHI and EcoRI and then inserted into pIEnGFP vector. The ORF of ESCRT-III components were isolated from Y-pMD18-T using restriction enzymes XbaI and EcoRI (Vps2B, Vps20, Vps24, Snf7, Vps46) or XbaI and PstI (Vps60),

195 then cloned into the same enzyme sites of pIEcGFP or pIE-MCS-Myc (44) to produce
196 the target genes fused with GFP or a c-Myc tag at the C-terminus. The HA- or c-Myc-
197 tagged AcMNPV genes (Ac11, Ac76, Ac78, GP41, Ac93, p48, Ac142, Ac146, Lef3)
198 expression plasmids and the mCherry-based bimolecular fluorescent complementation
199 (BiFC) system were constructed as described previously (44, 45). The gene specific
200 BiFC plasmids Y-HA-NmpBlue, Z-HA-NmpBlue, U-HA-NmpBlue, Y-Myc-CmpBlue, Z-
201 Myc-CmpBlue, U-Myc-CmpBlue (Y, Z, U, Nm, and Cm represents ESCRT-III
202 components, AcMNPV genes except Ac146, Vps4 and its mutants E231Q and K176Q,
203 the N- and C-termini of mCherry, respectively) were generated by insertion the XbaI-
204 EcoRI fragment isolated from Y-pMD18-T, pIE-Z-Myc, Vps4-gfppBlue, E231Q-gfppBlue,
205 K176Q-gfppBlue (23) into HA-NmpBlue or Myc-CmpBlue (44), respectively. Nm-
206 Ac146pBlue and Cm-Ac146pBlue were generated by insertion the PCR products of the
207 ORF of Ac146 digested with BamHI and EcoRI into Nm-HApBlue or Cm-MycpBlue (44),
208 respectively.

209 Recombinant AcMNPV bacmids expressing GFP, GFP-tagged ESCRT-I or ESCRT-
210 III components, or Vps4 mutant E231Q-GFP were constructed by inserting a cassette
211 containing GFP, GFP-tagged ESCRT-I or ESCRT-III components, or E231Q-GFP under
212 the control of the AcMNPV *ie1* immediate early promoter, into either a) a pFastbac
213 plasmid (GUSpFB) that contain a β-glucuronidase (GUS) gene under the control of the
214 AcMNPV *p6.9* late promoter, or b) a pFastbac plasmid (VP39-mCherrypFB) that contain
215 AcMNPV *vp39* gene fused with mcherry at its C-terminus under the control of *vp39*
216 native promoter. The resulting pFastbac constructs (GFPpFB, GFP-XpFB, Y-GFPpFB,
217 E231Q-GFPpFB, GFP-VP39-mCherrypFB, Y-GFP-VP39-mCherrypFB, E231Q-GFP-

218 VP39-mCherrypFB, X, Y represents ESCRT-I or ESCRT-III components, respectively)
219 were each inserted into the polyhedrin locus of an AcMNPV bacmid (bMON14272) by
220 Tn*7*-mediated transposition (46). The resulting recombinant bacmids were separately
221 named GFPBac, GFP-XBac, Y-GFPBac, E231Q-GFPBac, GFP-VP39-mCherryBac, Y-
222 GFP-VP39-mCherryBac, E231Q-GFP-VP39-mCherryBac. All constructs were confirmed
223 by restriction enzyme analysis and DNA sequencing. The control AcMNPV bacmid
224 AcMNPV-LacZGUS, *gp64* knockout AcMNPV bacmid LacZGUS-*gp64*^{ko} and
225 mCherryGUS-*gp64*^{ko} were constructed as described earlier (23). In these bacmids, the
226 expression of the reporter gene LacZ or mCherry is directed by an OpMNPV *ie2*
227 immediate early promoter, and GUS is directed by the AcMNPV *p6.9* late promoter. The
228 plasmids and bacmids were purified by using the Midiprep kit (Invitrogen). The *gp64*
229 knockout virus LacZGUS-*gp64*^{ko} and mCherryGUS-*gp64*^{ko} were grown and titred in
230 Sf9^{OP1D} cells. Wild-type AcMNPV encoding VP39-triple mCherry (3mC) was kindly
231 provided by Taro Ohkawa and Matthew Welch (University of California, Berkeley) (31).

232 **Infectivity complementation assay**

233 Sf9 cells and High 5 cells in 12-well plate were transfected with a total of 4 µg of
234 plasmid DNA per well comprising of 2 µg of pBieGP64 (47) expressing AcMNPV GP64
235 and 2 µg of plasmid encoding either GFP, GFP-tagged ESCRT-I or ESCRT-III
236 components, or E231Q-GFP. At 16 h posttransfection (p.t.), the cells were infected with
237 the *gp64* knockout AcMNPV virus mCherryGUS-*gp64*^{ko} (multiplicity of infection [MOI] =1
238 or 5) that produced in Sf9^{Op1D} cells(42). At 24 h p.i., the infected cells and medium were
239 collected separately. Infectious viruses in the medium were tittered by 50% tissue culture

infective dose ($TCID_{50}$) on $Sf9^{OP1D}$ cells. Cell samples were subjected to Western blot analysis.

RNAi assay

The dsRNA-based RNA interference (RNAi) assay was performed as described previously with modifications (44, 48). A fragment (305-495 bp) of the coding sequence of the components of ESCRT-I (Tsg101, Vps28) or ESCRT-III (Vps2B, Vps20, Vps24, Snf7, Vps46, and Vps60), Vps4, or GFP was amplified by PCR. PCR primers were designed with the SnapDragon tool (http://www.flyrnai.org/cgi-bin/RNAi_find_primers.pl) and each primer contained the T7 RNA polymerase promoter sequence (5'-TAATACGACTCACTATAGGG-3') at the 5'-end (Table 1). The PCR products were purified using QIAEXII Gel Extraction Kit (QIAGEN). The purified PCR products were used as templates to produce dsRNA by using the T7 RiboMAX™ Express RNAi System (Promega). The dsRNA products were purified with RNeasy Mini Kit (QIAGEN) and analyzed by 1.2% agarose gel electrophoresis.

Sf9 cells in 12-well plates were transfected with 7.5 μg of dsRNA targeting the individual gene of ESCRT-I, ESCRT-III, or Vps4. Also, 7.5 μg of the GFP dsRNA was transfected as a negative control. The cell viability was determined using the CellTiter96@ AQueous One Solution Cell Proliferation Assay (MTS, Promega) according to the manufacturer's recommendations. Briefly, at 24, 48, and 72 h p.t., the cells were incubated with CellTiter 96® AQueous One Solution reagent for 2 h at 27° and absorbance at 490 nm was monitored using a 96-well plate reader (Tecan iControl Reader, Mannedorf, Switzerland). The specific gene expression knockdown efficiency was determined by transfecting Sf9 cells with 1 μg of the plasmid expressing HA-tagged

ESCRT-I, c-Myc-tagged ESCRT-III components, or Vps4, in combination with either 7.5 μg of dsRNA individually targeting a component of ESCRT-I, ESCRT-III, or Vps4, or 7.5 μg dsRNA of GFP as a control dsRNA. At 48 h p.t., the transfected and co-transfected cells were collected and the expression of each of the HA- or c-Myc-tagged ESCRT-I, ESCRT-III, or Vps4 proteins was determined by Western blotting. Western blots were quantified by using Quantity One software. For analysis of virus infection, Sf9 cells were transfected with 7.5 μg of dsRNA targeting the components of ESCRT-I, ESCRT-III, or Vps4, or 7.5 μg of the GFP dsRNA. At 48 h p.t., the transfected cells were infected with control AcMNPV at an MOI of 5. At 24 h p.i., the supernatants were collected and virus titers were measured by $TCID_{50}$ assays on Sf9 cells.

Analysis of viral gene expression and DNA replication

To determine the effects of dominant-negative ESCRT-I and ESCRT-III proteins on viral gene expression, Sf9 cells in a 12-well plate was co-transfected with 2 μg of pBieGP64 and 2 μg of the plasmid expressing GFP, or GFP-tagged ESCRT-I or ESCRT-III proteins. At 16 h p.t., the cells were infected with the *gp64* knockout virus AcMNPV LacZGUS-*gp64*^{ko} at an MOI of 5. At 6 and 24 h p.i., the infected cells were fixed and stained, or lysed and reporter proteins were quantified as described previously (23). Briefly, the infected cells were washed once with PBS (pH 7.4), fixed with 2% paraformaldehyde and 0.2% glutaraldehyde in PBS (pH 7.4) for 10 min, then washed twice with PBS, and permeabilized with a solution of 2 mM $MgCl_2$, 0.01% deoxycholate, and 0.1% Nonidet P-40 (NP-40), for 15 min. The fixed and permeabilized cells were then stained with the beta-Gal substrate X-Gal (5-bromo-4-chloro-3-indolyl-β-D-galactopyranoside, Gold Biotechnology) or stained with the GUS substrate X-gluc (5-

286 bromo-4-chloro-3-indolyl-β-D-glucuronic acid, Gold Biotechnology). Alternatively, the
287 infected cells were solubilized in PBS containing 0.5% NP-40 and beta-Gal or GUS
288 activities were quantified using the substrate Chlorophenol red-β-D-galactopyranoside
289 (CPRG, Roche Diagnostics GmbH) or 4-Nitrophenyl β-D-glucuronide (PNPG, Sigma-
290 Aldrich) and spectrometry (O.D. 570nm or 405nm, respectively).

291 To examine the effect of dominant-negative ESCRT-I and ESCRT-III proteins on viral
292 DNA replication, real-time PCR was performed as described previously (23). In brief, Sf9
293 cells were co-transfected with 2 μg of pBieGP64 and 2 μg the plasmid expressing GFP,
294 or GFP-tagged ESCRT-I or ESCRT-III proteins. At 16 h p.t., cells were infected with the
295 *gp64* knockout virus LacZGUS-*gp64*^{ko} (MOI=5). At 24 h p.i., the infected cells were
296 harvested and the total DNA was extracted with a DNeasy® Blood&Tissue kit (QIAGEN).
297 The viral genomic DNA was determined by real-time PCR (23). Each PCR reaction
298 mixture contained 5 μl SYBR Green PCR master mix (TaKaRa), 1.25 μM of each primer
299 (forward primer: 5'-GATCTTCCTGCGGGCCAAACACT-3'; reverse primer: 5'-
300 AACAAGACCGCGCCTATCAACAAA-3'), and 300 pg of the total DNA. A 183 bp
301 fragment of the AcMNPV ODV-e56 gene was amplified by PCR. A control plasmid ODV-
302 e56pGEM-T containing the ORF of ODV-e56 was used to generate the standard curve.
303 The amount of AcMNPV genomic DNA was calculated and expressed as the number of
304 viral DNA copies in each cell.

305 **Analysis of virus entry**

306 For analysis of the effects on virus entry of overexpressing of ESCRT-I and ESCRT-
307 III components, or RNAi knockdown of ESCRT-I and ESCRT-III proteins, one set of Sf9
308 and High 5 cells in 12-well plates were transfected with 2 μg of the plasmid expressing

GFP, GFP-tagged ESCRT-I and ESCRT-III components, or E231Q-GFP. The other set of Sf9 cells in 12-well plates were transfected with 7.5 μg dsRNA targeting the component of ESCRT-I, ESCRT-III, Vps4, or the control GFP gene. At 16 h p.t. (for cells transfected with the plasmid) or 48 h p.t. (for cells transfected with dsRNA), the transfected cells were chilled at 4° for 45 min and then inoculated with pre-chilled control AcMNPV (MOI=10 $TCID_{50}$) or 3mC virus (MOI=20 $TCID_{50}$). After 1 h attachment at 4°, the viral inoculum was removed and the cells were washed twice with chilled TNMFH medium and shifted to 27° in TNMFH medium. After incubation at 27° for 90 min, the wild-type AcMNPV-infected cells were collected and the amount of viral genomic DNA was measured by real-time PCR using the same primers and conditions as described above, and expressed as viral DNA genome copies per cell. The 3mC virus-infected cells were fixed with 3.7% paraformaldehyde in PBS (pH7.4) and examined by confocol microscopy as described below.

Analysis of infectious AcMNPV production and release

For analysis of overexpression or knockdown of ESCRT-I and ESCRT-III components on infectious AcMNPV release, one set of Sf9 and High 5 cells in 6-well plates were transfected with recombinant AcMNPV bacmid DNA (6 μg per well) expressing either GFP, GFP-tagged ESCRT-I or ESCRT-III, or E231Q-GFP. The other set of Sf9 cells in 12-well plates were transfected with 7.5 μg dsRNA targeting the component of ESCRT-I, ESCRT-III, Vps4 or GFP and were transfected again at 48 h p.t. with 3 μg AcMNPV bacmid DNA (AcMNPV-LacZGUS). After transfection with AcMNPV bacmid DNA and incubation for 24 h, the GFP-positive cells in first set of transfected Sf9 and High 5 cells were scored by epifluorescence microscope (Nikon Eclipse Ti) to

estimate the transfection efficiency, and wells containing more than 1×10^4 cells were selected for analysis. Also, two sets of the transfected cells were lysed and GUS (in the first set of transfected cells) or beta-Gal and GUS (in the second set of transfected cells) activities were quantified as described above. For each transfection, the cell culture medium from 3 wells of transfected cells was collected and centrifuged (3000 x *g*, 10 min, 4°) to remove the cellular debris. Infectious virus titres were determined by $TCID_{50}$ assays on Sf9 or High 5 cells. To track the effects of overexpression of ESCRT-III components Vps24, Snf7, and Vps60, and Vps4 mutant E231Q on budded virions release, Sf9 cells in 6-well plates were transfected with AcMNPV bacmid DNA (6 µg per well) expressing VP39-mCherry and either GFP, Vps24-GFP, Snf7-GFP, Vps60-GFP or E231Q-GFP (GFP-VP39-mCherryBac, Vps24-GFP-VP39-mCherryBac, Snf7-GFP-VP39-mCherryBac, Vps60-GFP-VP39-mCherryBac, and E231Q-GFP-VP39-mCherryBac, respectively). At 24 h p.t., the transfected cells were fixed with 3.7% paraformaldehyde in PBS (pH7.4) and examined by confocal microscopy as described below.

Confocal microscopy

Sf9 or High 5 cells that were plated on glass coverslips and transfected and/or infected, were fixed with 3.7% paraformaldehyde in PBS (pH 7.4) for 10 min. Cells were then washed three times with PBS (pH 7.4) and permeabilized with 0.05% Triton X-100 in PBS (pH 7.4). The nuclei were stained with 1 µg/ml Hoechst 33258 (Invitrogen) for 8 min. After washing three times with PBS (pH 7.4), the cells were mounted on slides in Fluoromount-G™ reagent (Southern Biotech). Images were collected on a Nikon A1R+ confocal microscope (Nikon Instruments Inc., Melville, NY, USA) using a 63x oil

355 immersion objective NA 1.4. GFP was excited with a blue argon ion laser (488 nm), and
356 emitted light was collected between 480 nm and 520 nm. mCherry was excited with an
357 orange helium-neon laser (594 nm), and emitted light was collected from 580 nm to 650
358 nm. Hoechst 33258 was excited with ultraviolet light at app 350 nm, and emitted light
359 was collected from 400 nm to 450 nm. GFP and mCherry signals were collected
360 separately from the Hoechst 33258 signal and later superimposed. Images were
361 processed using NIS-Elements Viewer software (version 4.0) and Adobe Photoshop CS5
362 (Adobe systems).

363 **Transmission electron microscopy (TEM)**

364 Sf9 cells in 6-well plates were transfected with AcMNPV bacmid DNA (6 μg per well)
365 expressing VP39-mCherry and either GFP, Vps24-GFP, Snf7-GFP, Vps60-GFP or
366 E231Q-GFP (GFP-VP39-mCherryBac, Vps24-GFP-VP39-mCherryBac, Snf7-GFP-
367 VP39-mCherryBac, Vps60-GFP-VP39-mCherryBac, and E231Q-GFP-VP39-
368 mCherryBac, respectively). At 72 h p.t., the transfected cells were harvested by
369 centrifugation (500 *g*, 10 min) and fixed with 2.5% glutaraldehyde in PBS (pH 7.4) at 4°
370 overnight. Then, the cells were washed five times with PBS buffer (0.1 M, pH 7.2) and
371 stained with 1% osmium tetroxide in PBS buffer (0.2 M, pH 7.2) for 2 h at 4°. After
372 washing five times in PBS buffer (0.1 M, pH 7.2), the fixed cells were dehydrated with a
373 gradient of ethanol from 30% to 100%. The cells were then embedded in Epon-812 and
374 dried for 48 h at 55°. Ultrathin sections were prepared and stained with lead citrate and
375 uranyl acetate. Images were collected using the HT7700 transmission electron
376 microscope (Hitachi, Ltd. Japan).

Syncytium formation and cELISA analysis

Sf9 cells in each well of a 6-well plate were transfected with 6 μg of a bacmid expressing GFP, GFP-tagged ESCRT-III components, or E231Q-GFP. At 24 h p.t., one set of the transfected cells were incubated with PBS at pH 5.0 for 3 min to induce syncytium formation, and another set of the transfected cells were used to quantify the cell surface level of the major viral envelope protein GP64 by cell surface enzyme-linked immunosorbent assay (cELISA). The syncytium formation and cELISA analyses were carried out as described previously (47, 49). Briefly, in syncytium formation assay, Sf9 cells were fixed with methanol and stained with 0.1% Eosin Y and 0.1% methylene blue. For cELISA analysis, Sf9 cells were fixed in 0.5% glutaraldehyde and the relative levels of GP64 localized at the cell surface were measured using primary MAb AcV5, a secondary goat anti-mouse antibody conjμgated to beta-galactosidase, and the substrate chlorophenol red-beta-D-galactopyranoside (CPRG).

Coimmunoprecipitation

Sf9 cells in 12-well plates were transfected or co-transfected with the plasmids expressing c-Myc tagged ESCRT-III components, Vps4 or viral proteins or HA-tagged viral proteins (2 μg DNA for each plasmid). At 36 h post-transfection, the cells were lysed in RIPA buffer (0.1% SDS, 50mM Tris pH 8.0, 150 mM NaCl, 5mM EDTA, 0.5% Sodium deoxycholate, 1% NP-40) containing protein inhibitor cocktail (Roche) and the supernatant was collected after centrifugation (15,000 x *g*, 15 min, 4°). For immunoprecipitation, the lysate supernatants were mixed with Protein G agarose beads (Pierce) and anti-HA monoclonal antibody (MAb) overnight at 4°. After pelletting and washing twice with RIPA buffer, the agarose beads were resuspended with 1×SDS gel

loading buffer (2% SDS, 10% glycerol, 2% 2-mercaptoethanol, 0.02% bromophenol blue, 0.05 M Tris, pH 6.8) and analyzed in 10% or 15% SDS-PAGE and Western blot.

Bimolecular fluorescent complementation (BiFC) assay

Sf9 cells in 12-well plate were co-transfected with the BiFC pair plasmids (2 μg DNA for each construct). At 36 h p.t., bimolecular fluorescent complementation was assessed by imaging mCherry fluorescence in transfected Sf9 cells expressing pairs of N-terminal or C-terminal gene fusions to either the N- or C-terminus of mCherry (Nm or Cm, respectively). Fluorescence was observed with a Nikon Eclipse Ti epifluorescence microscope. The fluorescent cells in five randomly selected representative fields were scored for each pair constructs. The pair proteins interaction was evaluated as described previously (5) by the ratio of the number of fluorescent cells in one field with the total number of cells in that field. The transfected cells were also collected for Western blot analysis of the target proteins expression.

Western blot analysis

Proteins were separated by 10% or 15% SDS-PAGE and transferred to PVDF membrane (Millipore). GFP and GFP-tagged proteins were detected on Western blots with an anti-GFP polyclonal antibody (GenScript), HA- or c-Myc-tagged proteins were detected with anti-HA MAb or an anti-Myc polyclonal antibody (GenScript), and GP64 or actin were detected using MAb AcV5 (Santa Cruz Biotechnology) or anti-β-actin monoclonal antibodies (Abbkine). Immunoreactive proteins were visualized using alkaline phosphatase-conjugated anti-mouse or anti-rabbit IgG antibody and nitroblue tetrazolium/5-bromo-4-chloro-3-indolylphosphate (NBT/BCIP; Promega).

Accession numbers

The *Spodoptera frugiperda* ESCRT-I components Vps23/Tsg101 and Vps28, and ESCRT-III components Vps2B, Vps20, Vps24, Vps32/Snf7, and Vps60 genes were deposited under GenBank accession numbers: KY694523, KY694524, KY694525, KY694526, KY694527, KY694528, KY694529.

Results

Isolation of ESCRT-I and ESCRT-III components from Sf9 cells

Using the *Spodoptera frugiperda* EST sequence database (SPODOBASE) to identify homologs of yeast ESCRT-I and ESCRT-III components, we identified full-length cDNA sequences for Vps2B, Vps20, Vps28, Vps46, Vps60, and Snf7. We also identified 5' and 3' ends partial sequences for Vps23 (Tsg101 in mammalians) and only 5' end sequence for Vps24. To confirm and subclone cDNAs of these ESCRT components from *Spodoptera frugiperda* Sf9 cells, we initially designed gene-specific primers targeted to the 5' upstream and 3' downstream untranslated sequences. For Vps24, the sequence of the 3' end of the gene was obtained by 3' RACE. We then designed gene-specific primers containing unique restriction enzyme sites to amplify the ORF for each component of ESCRT-I and ESCRT-III complexes (listed above). Nucleotide sequence analysis revealed several nucleotide sequence errors in the SPODOBASE sequences, resulting in frame shift or same sense mutations within the original EST sequences. cDNA sequences for these mRNAs were deposited into GenBank.

Amino acid sequence alignments revealed that the components of ESCRT-I and ESCRT-III from Sf9 cells have a high level of identity to their homologs from other insects, yeast and humans (Fig. S1). In mammalian cells, there are multiple isoforms of ESCRT-III components, including CHMP1 (CHMP1A, B; homologs of yeast Vps46), CHMP2 (CHMP2A, B; homologs of yeast Vps2), and CHMP4 (CHMP4A, B, and C; homologs of yeast Snf7) (isoforms are in listed in parenthesis). In insects, gene expansion was only observed for Vps2 (Vps2A, B) in lepidopteran and a few other species. Most of the sequenced insect genomes contain only a single ortholog of Vps2

(40). Here, we identified a single ortholog of Vps2 from Sf9 cells, and that ortholog is most similar to human CHMP2B, and Vps2B from other insects. Thus, we designated this single identified Sf9 Vps2 gene as Vps2B. Additionally, the N-terminal ubiquitin-enzyme variant (UEV) domain, middle region proline-rich region (PRD) and coiled coil (CC), and the C-terminal steadiness box (SB) of Tsg101/Vps23 (Fig. S1, Tsg101/Vps23), and the N-terminal core region and the C-terminal four helix bundle domain (CTD) of Vps28 (Fig. S1, Vps28) are highly conserved among insect, yeast, and humans. All of the isolated ESCRT-III components of Sf9 contain a predicted Snf7 domain of about 170 amino acids (Fig. S1).

Expression of wild-type and dominant-negative ESCRT-I and ESCRT-III components

It was previously shown that overexpression of Tsg101 lacking one of its subdomains (UEV, PRD, CC, or SB) results in dominant-negative inhibition of HIV-1 budding (50-52). Also, mutations within the CTD domain of Vps28 (that disrupt interaction of Vps28 and ESCRT-III component Vps20) result in lower efficiency budding by equine infectious anaemia virus (EIAV) Gag (53). To generate predicted dominant-negative forms of Sf9 ESCRT-I components Tsg101 and Vps28, we generated constructs of Sf9 Tsg101 (Fig. 1A) consisting of residues 1 to 160 (UEV, UEV domain), 150 to 403 (dUEV, deletion of UEV domain), 250 to 403 (CC-SB, deletion of UEV and PRD domains), 330 to 403 (SB, SB domain), and a construct called Core, which lacks the C-terminal domain (CTD) of Vps28. Wild-type and modified forms of Tsg101 and Vps28 were N-terminally tagged with GFP. Dominant-negative forms of Sf9 ESCRT-III components were generated by fusing a GFP tag to the C-terminus of each. As described previously, the C-terminus of

473 ESCRT-III components serve as the auto-inhibitory element that interacts with the N-
474 terminal portion and maintains ESCRT-III components as monomers in the cytoplasm.
475 Release of the inhibitory effect of the C-terminus is required for ESCRT-III assembly (54-
476 56). In yeast and mammalian cells, fusion of a bulky tag such as GFP to the C-terminus
477 of ESCRT-III components interferes with the auto-inhibition and results in the dominant-
478 negative phenotype (57, 58). Each fusion construct was transiently expressed in Sf9
479 cells under the control of an AcMNPV *ie1* promoter and detected by Western blot
480 analysis with an anti-GFP antibody and by epifluorescence microscopy (Fig. 1B, C, 2B,
481 C).

482 ESCRT-I components. Transient expression of full-length Tsg101 resulted in a highly
483 punctate, putatively endosomal pattern of expression (Fig. 1C, Tsg101). In contrast,
484 expression of the N-terminal UEV domain, or the C-terminal SB domain of Tsg101,
485 resulted in GFP-tagged proteins that were distributed diffusely throughout the cytoplasm
486 and nucleus, even though a small portion of the proteins from these modified constructs
487 (especially SB) had a punctate distribution in the cytoplasm (Fig. 1A and C; UEV, SB).
488 Transient expression of dUEV and CC-SB (both lacking the N-terminal UEV domain)
489 resulted in formation of large, apparently spherical structures in the cytoplasm. GFP-
490 Vps28 exhibited a diffuse pattern of localization in both the nucleus and the cytoplasm
491 (Fig. 1C, Vps28). Deletion of the C-terminal CTD domain of Vps28 did not alter the
492 distribution of Vps28. However, transient expression of the Vps28 without the CTD
493 appears to induce the formation of vacuoles in Sf9 cells (Fig. 1C, Core, see phase
494 image).

ESCRT-III components. For ESCRT-III components (Fig. 2), Vps20-GFP was localized diffusely in the cytoplasm and induced a low occurrence of vacuoles (Fig. 2C, Vps20). In contrast, when the other ESCRT-III components were GFP-tagged, they accumulated in punctate structures in the cytoplasm and a significantly high level of cytoplasmic vacuolation was observed (Fig. 2C, phase panels).

Previous studies indicated that overexpression of a dominant-negative form of Sf9 Vps4 (an ATP hydrolysis defective form of Sf9 Vps4, E231Q-GFP) induced the formation of an aberrant endosomal compartment (23). To determine whether the compartment induced by Vps4 E231Q resembled that induced by overexpression of the wild-type or dominant-negative forms of ESCRT-I and ESCRT-III components, we co-transfected Sf9 cells with two plasmids: one expressing Vps4 E231Q-mCherry, and another expressing each construct of ESCRT-I and ESCRT-III, and we then examined the localization of the two proteins (DN Vps4 and ESCRT -I or -III constructs). Complete colocalization was observed between Vps4 E231Q-mCherry and GFP-tagged ESCRT-III components, Vps2B, Vps24, Snf7, Vps46, or Vps60 , and majority of the GFP-tagged Vps20 was also observed to be colocalized with E231Q-mCherry (Fig. 2D). In contrast, no colocalization was observed between Vps4 E231Q-mCherry and wild-type Tsg101 or the truncated forms of Tsg101: dUEV or CC-SB (Fig. 1D). Additionally, coexpression with Vps4 E231Q-mCherry did not change the localization pattern of modified forms of Tsg101 (UEV and SB), Vps28, and Vps28 core domain (Core) (Fig. 1C vs 1D). These results suggested that overexpression of GFP-tagged ESCRT-III components resulted in formation of the aberrant endosomal compartment similar to that induced upon Vps4 E231Q-mCherry expression, or that coexpression of Vps4 E231Q-mCherry and

components of ESCRT-III results in the retention of both of the proteins in the same aberrant endosomal compartment.

ESCRT-I and ESCRT-III components are required for production of infectious AcMNPV BV

To first ask whether the components of ESCRT-I and ESCRT-III are required for production of AcMNPV BV, we initially used a viral complementation assay to examine viral replication in transfected-infected cells (Fig. 3A). Because all cells do not become transfected and express the constructs of ESCRT-I and ESCRT-III in transient transfection assays, the complementation assay insures that productive viral replication can occur only in cells that are productively transfected and express both of the constructs of ESCRT-I or ESCRT-III and AcMNPV GP64 (which complements infection by a *gp64* knockout virus and permits production of infectious BV) (Fig. 3A, b). In this assay, Sf9 cells were initially co-transfected with two plasmids separately expressing the essential viral envelope protein GP64 and a GFP-tagged ESCRT-I or ESCRT-III protein. After a 16 h period of expression, the cells were infected with the *gp64* knockout virus mCherryGUS-*gp64*^{ko} that produced in Sf9^{Op1D} cells (the reporter genes mCherry and GUS are controlled by the OpMNPV *ie2* immediate early promoter and AcMNPV *p6.9* late promoter, respectively). Supernatants were harvested at 24 h postinfection (p.i.) and infectious AcMNPV BV titers were determined by $TCID_{50}$ assays on Sf9^{OP1D} cells that stably express of OpMNPV GP64. Sf9 cells co-transfected with plasmids expressing GP64 and GFP served as a negative control, whereas co-transfection of cells with plasmids expressing the dominant-negative Vps4 construct, Vps4 E231Q-GFP, and

GP64 (which result in dramatically reduced infectious virus titers) served as a positive control for inhibition of AcMNPV production (23).

The overexpression of full-length GFP-tagged ESCRT-I components Tsg101 and Vps28 significantly reduced the production of infectious AcMNPV, with reductions of approximately 85-90% (Fig. 3B). The reduction in BV titer was typically more severe in the presence of the truncated forms of Tsg101 and Vps28 and that effect was more clearly evident when infections were performed at MOI 1 (Fig. 3B). Dominant-negative ESCRT-III components also caused a substantial inhibition in BV production, with the majority of ESCRT-III constructs reducing the infectious BV titers to <10% of the control (Fig. 3C). The most dramatic reduction in BV production (approximately 98%) was detected in cells expressing of Vps24-GFP (Fig. 3C). Western blot analysis showed that GP64 and each of the ESCRT-I and ESCRT-III constructs were expressed at similar levels in transfected-infected cells (Fig. 3D) indicating that variations in transiently expressed proteins were not responsible for the observed effects. In addition, when parallel experiments were performed in another lepidopteran cell line (*Trichoplusia ni* High5 cells; data not shown) similar reductions in BV production were also observed.

To extend our observations, we used a dsRNA-based RNAi approach to knockdown the expression of individual component of ESCRT-I or ESCRT-III, or Vps4 and evaluated the effect on infectious AcMNPV production. Sf9 cells were mock transfected or transfected with dsRNA targeting the specific component of ESCRT-I or ESCRT-III, or Vps4, or a dsRNA targeting GFP. Knockdown efficiencies were ranged from 71.5 to 94.3% (Fig. 4A), and transfection with the dsRNA of the ESCRT components or GFP caused no notable change in the viability of Sf9 cells at 24, 48, and 72 h p.t. (data not

shown). Similarly, we observed that knockdown of individual components of ESCRT-I (Tsg101, Vps28) or ESCRT-III (Vps2B, Vps20, Vps24, Snf7, Vps46, Vps60), or Vps4 resulted in a dramatic reduction of infectious AcMNPV production (Fig. 4B).Taken together, these results suggest that when cells are infected with BV, functional ESCRT-I and ESCRT-III complexes are required for production of infectious AcMNPV BV progeny.

Overexpression of ESCRT-I and ESCRT-III components affect early stages of AcMNPV infection

Since AcMNPV budded virions enter host cells by clathrin-mediated endocytosis (28), the inhibitory effect of GFP-tagged ESCRT-I and ESCRT-III proteins on AcMNPV infection could occur at an early stage of virus infection, by inhibiting virus entry or transport to the cell nucleus. To address this possibility we used the same virus complementation system described above, but with a virus that expresses early and late phase reporter genes. Sf9 cells were first co-transfected with two plasmids expressing: a) GP64 and b) one of the ESCRT-I or ESCRT-III constructs, or the control GFP or control Vps4 E231Q-GFP. At 16 h post transfection (h p.t.), the co-transfected cells were infected with a *gp64* knockout virus (LacZGUS-*gp64*^{ko}), which contains the reporter genes: LacZ (beta-galactosidase) under an AcMNPV *ie1* early promoter, and GUS (beta-glucuronidase) under the AcMNPV *p6.9* late promoter. We used these two reporter genes to monitor early and late events in the AcMNPV infection cycle. In comparison with the GFP control, we found that the expression of full-length or truncated forms of ESCRT-I proteins (Tsg101 and Vps28), or dominant-negative forms of ESCRT-III proteins significantly decreased the beta-Gal and GUS positive cells (data not shown). In the transfected-infected cell lysates, the activities of beta-Gal and GUS were generally

suppressed by more than 35%-60%, by expressing these ESCRT-I and -III constructs (Fig. 5A-D). Both Vps2B-GFP and Snf7-GFP reduced the detection of the late reporter (GUS) to a level similar to that of the control Vps4 DN construct (E231Q-GFP) (Fig. 5D). To confirm these results, we further examined viral DNA replication in Sf9 cells co-transfected with the above plasmids and infected with the *gp64* knockout virus (LacZGUS-*gp64*^{ko}, MOI 5). Viral genomic DNA was extracted at 24 h p.i. and analyzed by quantitative real-time PCR. Consistent with the reporter gene expression results, viral genomic DNA was substantially reduced in cells expressing full-length or dominant-negative proteins of ESCRT-I and ESCRT-III (Fig. 5E, F). Overall, these data suggest that overexpression of GFP-tagged full-length or truncated forms of ESCRT-I and ESCRT-III proteins in Sf9 cells interfere with AcMNPV infection at an early stage such as virus entry or transport to the cell nucleus.

ESCRT-I and ESCRT-III components are required for efficient AcMNPV budded virion entry

During endocytosis, trafficking, and multivesicular body formation, ESCRT-I is required for cargo sorting and promoting membrane curvature. In contrast, ESCRT-III functions at a late step to catalyze scission and membrane fission (1, 6) to release the newly-formed vesicle. To determine whether ESCRT-I and ESCRT-III are important for AcMNPV internalization or transport during entry, we used two strategies: 1) overexpression of GFP-tagged ESCRT-I and ESCRT-III proteins, and 2) RNAi knockdown of individual components of ESCRT-I and ESCRT-III. For these studies, one set of Sf9 cells was transfected with a plasmid expressing GFP-tagged ESCRT-I or ESCRT-III proteins, or the control GFP or E231Q-GFP, the other set of Sf9 cells was

609 transfected with dsRNA targeting the component of ESCRT-I or ESCRT-III, or Vps4 or
610 the control GFP. At 16 h p.t. (for the first set cells transfected with plasmids) or 48 h p.t.
611 (for the second set of cells transfected with dsRNA), the cells were chilled at 4° and
612 infected with control AcMNPV (AcMNPV-LacZGUS) or a previously described AcMNPV
613 virus (AcMNPV-3mC) that contains an mCherry-tagged major capsid protein VP39
614 (VP39-mCherry). After low temperature binding to cells for 1 h, the infected cells were
615 incubated at 27° for 90 min to allow the viruses to enter cells. To quantitatively analyze
616 viruses that had entered the cell, DNA was extracted from control AcMNPV infected cells
617 and viral genomic DNA was quantified by real-time PCR. As shown in Figure 6 and 7,
618 viral genomic DNA levels were substantially decreased in cells expressing the dominant-
619 negative Vps4 protein, E231Q-GFP (Fig. 6A, B) or in cells with an RNAi knockdown of
620 Vps4 (Fig. 7A). Cells transfected with the dominant-negative constructs of ESCRT-III
621 (Fig. 6B) or cells transfected with dsRNA targeting specific ESCRT-III components (Fig.
622 7A) also showed a similar reduction of viral genomic DNA. In contrast, prior expression
623 of full-length or truncated forms of ESCRT-I proteins Tsg101 or Vps28, or targeted
624 knockdown of Tsg101 or Vps28, did not appear to affect the amount virus that entered
625 the cells (Fig. 6A, 7A). To track virion entry more directly, cells infected with the
626 AcMNPV-3mC virus were analyzed by confocal microscopy. As shown in Figure 6C and
627 7B, entering mCherry labeled nucleocapsids (NCs) are found distributed uniformly in the
628 cytoplasm of cells transiently expressing control GFP or cells transfected with the dsRNA
629 of GFP and some virus particles were observed in the nucleus of cells. In contrast,
630 similar to that observed for Vps4 E231Q-GFP, virus NCs were mostly observed
631 aggregated within the cytosol in cells expressing the constructs of ESCRT-I and ESCRT-

III (Fig. 6C) or in cells transfected with dsRNA specific for components of ESCRT-I, ESCRT-III, or Vps4 (Fig. 7B)., Similar results were also observed in parallel experiments using High5 cells expressing GFP-tagged ESCRT-I and ESCRT-III proteins (data not shown). Together, these data indicate that during AcMNPV BV entry, the ESCRT-I complex is required for virion or nucleocapsid trafficking, whereas the ESCRT-III complexe is required for efficient internalization and transport of virions.

ESCRT-III but not ESCRT-I components are required for efficient egress of infectious AcMNPV

As described above, overexpression of GFP-tagged forms or knockdown of the ESCRT-I or ESCRT-III components substantially impaired virion entry and transport of nucleocapsids to the nuclei of cells. Therefore, to avoid this negative effect and ask whether ESCRT-I and ESCRT-III are also required for efficient budding of AcMNPV, we used two strategies: 1) viral bacmid DNA expressing GFP-tagged ESCRT proteins was used to transfect cells to eliminate virion entry effects, and 2) RNAi knockdowns were used in addition to overexpression of WT and dominant-negative constructs. For first strategy, Sf9 cells were infected by transfecting cells with AcMNPV bacmid DNAs that individually express a GFP-tagged ESCRT-I or ESCRT-III protein, plus a reporter GUS protein. In each bacmid, the ESCRT component was expressed under the *ie1* early promoter and GUS was expressed under a *p6.9* late promoter. For the second strategy, Sf9 cells were transfected with the dsRNA specific for the component of ESCRT-I or ESCRT-III, and at 48 h p.t., the cells were transfected again with control AcMNPV bacmid DNA that contains the reporter genes LacZ and GUS under the OpMNPV *ie2* early promoter and the AcMNPV *p6.9* late promoter, respectively. For both strategies,

after transfection with the bacmid DNAs and incubation for 24 h, we determined the GFP fluorescence, or beta-Gal and GUS activities to evaluate the transfection efficiencies and monitor progression of the virus infection, respectively. In the first strategy, the percentage of GFP-positive cells at 24 h p.t. ranged from 30.4 to 37.5% (Fig. 8A), and GUS activities at 24 h p.t. were similar among cells transfected with the different bacmids (Fig. 8B). For cells transfected with dsRNA and the AcMNPV-LacZGUS bacmid, the beta-Gal and GUS activites were similar (Fig. 9A, B). These results indicated that the transfection efficiencies for different bacmids or for the control AcMNPV bacmid and various dsRNAs, were equivalent and the virus infection cycle progressed into the late phase of infection. As shown in Figure 8C and 9C, the expression of full-length and truncated forms of ESCRT-I components Tsg101 or Vps28 or knockdown the expression of these two components did not reduce infectious virus titers compared to the GFP control. Similarly, the expression of the ESCRT-III construct Vps20-GFP (Fig. 8C) or the Vps20 knockdown (Fig. 9C) had no substantial effect on levels of infectious virus produced. In contrast however, the expression of the other two dominant-negative ESCRT-III proteins (Vps24 and Snf7) (Fig. 8C, ESCRT-III) and the corresponding Vps24 and Snf7 knockdowns (Fig. 9C) resulted in a strong inhibition of infectious AcMNPV BV production (> 650 fold) similar to the reduction observed when dominant-negative Vps4 construct E231Q-GFP was expressed or when Vps4 was knocked down by RNAi (Fig. 8C, 9C). Virus titers were also reduced substantially in supernatants from cells expressing Vps2B-GFP, Vps46-GFP, or Vps60-GFP, and from cells with RNAi knockdowns of Vps2B, Vps46, or Vps60 (Fig. 8C, 9C). Similar results

677 were observed in *T. ni* High5 cells expressing DN forms of ESCRT-III proteins (data not
678 shown).

679 Since the viral envelope glycoprotein GP64 is important for budding and release of
680 BV (33), the effect of dominant-negative ESCRT-III proteins on infectious BV production
681 might result from the disruption of transport or cell surface localization of GP64. To
682 examine this possibility, Sf9 cells transfected with AcMNPV bacmids expressing GFP,
683 GFP-tagged ESCRT-III proteins, or Vps4 E231Q-GFP (as described above) were fixed
684 at 24 h p.t., and relative cell surface levels of GP64 were analyzed by cELISA. In the
685 presence of DN ESCRT-III proteins or Vps4 E231Q, cell surface levels of GP64 were
686 similar to that observed in the presence of control GFP protein (data not shown).
687 Analysis of syncytium formation also revealed that, in the presence of dominant-negative
688 ESCRT-III proteins or Vps4 E231Q, GP64 efficiently induced membrane fusion (data not
689 shown). These results suggested that DN ESCRT-III proteins and Vps4 E231Q had no
690 apparent effect on transport or cell surface localization and membrane fusion activity of
691 GP64. Together, these data provide evidence that ESCRT-III is required for efficient
692 egress of infectious AcMNPV, and that effect does not appear to result from a defect in
693 GP64 transport.

694 **ESCRT-III/Vps4 is involved in nuclear egress of nucleocapsids of AcMNPV**

695 During viral egress of BV, progeny nucleocapsids of AcMNPV (which assemble in the
696 nucleus) cross the nuclear membrane and are transported to the plasma membrane.
697 There, nucleocapsids bud and virions pinch off to form infectious budded virus or BV (25).
698 The inhibitory effect of RNAi or dominant-negative ESCRT-III and Vps4 on infectious
699 AcMNPV BV release could result from defect(s) in nucleocapsid egress across the

700 nuclear membrane, transport through the cytoplasm, and/or budding and fission at the
701 plasma membrane. To track nucleocapsid release, Sf9 cells were transfected with
702 AcMNPV bacmids expressing mCherry-tagged major capsid protein VP39 (VP39-
703 mCherry), plus one of the following: Vps24-GFP, Snf7-GFP, Vps60-GFP, Vps4 E231Q-
704 GFP, or the control GFP. At 24 h p.t., the transfected cells were subjected to confocal
705 microscopy. In cells expressing Vps60-GFP, the Vps60 was found predominantly in the
706 cytoplasm. While mCherry-labeled nucleocapsids were found predominantly in the nuclei
707 as expected, we also observed a substantial amount of mCherry fluorescence in the
708 cytosol, suggesting detection of substantial amounts of NCs in the cytoplasm (Fig. 10,
709 Vps60-GFP). In contrast, mCherry-labeled VP39 appeared notably absent in the
710 cytoplasm of cells expressing Vps24-GFP, Snf7-GFP, or E231Q-GFP (Fig. 10, mCherry
711 column), suggesting that the inhibitory effect of dominant-negative ESCRT-III proteins
712 and Vps4 on infectious AcMNPV production during release may result from blocking
713 progeny nucleocapsid egress through or from host cell nuclear membranes. It was of
714 note additionally, that mCherry-labeled VP39 also appears to colocalize with Vps60-GFP
715 at or near the apparent nuclear ring zone region (Fig. 10, Vps60-GFP). To examine
716 these suggestive results in more detail, a parallel set of transfected cells was analyzed
717 by transmission electronic microscopy (TEM) at 72 h p.t. As shown in Fig. 11, we
718 observed a typical electronic-dense virogenic stroma (VS) and progeny nucleocapsids
719 had a normal morphology in cells expressing GFP, DN ESCRT-III constructs, or DN
720 Vps4 (Fig. 11A-E). Typical bundles of nucleocapsids were observed in the ring zone
721 region (white triangles), and progeny nucleocapsids were observed budding through the
722 nuclear membrane, in vesicles and free in the cytoplasm, and budding at the cytoplasm

membrane. Nucleocapsids in these locations were observed to varying degrees in the cells expressing the control GFP and DN ESCRT-III constructs (Fig. 11F). Numbers of nucleocapsids found in the post-nuclear locations (within the cytoplasm and budding at the cytoplasmic membrane) were substantially reduced in cells expressing Vps24-GFP and Snf7-GFP, and slightly reduced in Vps60-GFP expressing cells, as compared with cells expressing the control GFP (Fig. 11F). In Snf7-GFP expressing cells, we observed progeny nucleocapsids aggregated and localized in large spaces between inner and outer nuclear membranes (Fig. 11C). A similar defect in nucleocapsid budding was also observed in E231Q-GFP expressing cells (Fig. 11F). In addition, it was also noted that in Snf7-GFP and E231Q-GFP expressing cells, nuclecapsid bundles in the nuclear ring zone region were rarely observed (Fig. 11C, E). Together, our analysis of infectious virus release, mCherry-tagged nucleocapsid protein, and TEM of nucleocapsids suggest that the inhibitory effect of dominant-negative ESCRT-III constructs on infectious AcMNPV production may result from lower efficiency of progeny nucleocapsid egress from host cell nuclear membranes.

Interaction of ESCRT-III with viral proteins necessary for efficient budded virus production

A number of AcMNPV proteins (Ac11, Ac76, Ac78, Ac80 or GP41, Ac93, Ac103, Ac142, and Ac146) have been identified as important or essential for infectious budded virion production (34-39, 59, 60). Knockouts of these genes individually have no effect on viral DNA replication, but progeny nucleocapsids appear to be restricted to the nucleus in some or many cases, and egress from the nuclear membrane may be inhibited in many cases. Because the defects caused by these AcMNPV gene knockouts are similar to the

746 defects caused by dominant-negative ESCRT-III proteins, we hypothesized that some of
747 these viral proteins might interact with cellular ESCRT-III proteins. To address this
748 hypothesis, an immunoprecipitation assay was used to examine the potential interaction
749 between the components of ESCRT-III and each of the above viral proteins. We selected
750 AcMNPV GP41 and Lef3 as control proteins, as it was previously demonstrated that
751 GP41 interacts with itself but does not interact with Lef3 (61). For these interaction
752 studies, Sf9 cells were co-transfected with two plasmids: one plasmid expressing an HA-
753 tagged viral protein, and the another plasmid expressing a c-Myc epitope-tagged
754 ESCRT-III protein, GP41, or Lef3. Transfected cell lysates were used for
755 immunoprecipitation with anti-HA monoclonal antibody and protein G agarose. Western
756 blot analysis of the transfected cell lysates using anti-HA monoclonal antibody and anti-
757 Myc polyclonal antibody confirmed expression of each tagged viral and ESCRT-III
758 protein. HA-tagged viral proteins were immunoprecipitated with an anti-HA MAb, then
759 precipitates were challenged with an anti-Myc polyclonal antibody in Western blot
760 analysis. As described previously (61), GP41 co-immunoprecipitated with itself but not
761 with Lef3 (data not shown). Of the 8 viral proteins examined, we found that 6 (Ac11,
762 Ac76, Ac78, Ac80 or GP41, Ac93, and Ac146) co-immunoprecipitated with all or most of
763 the components of ESCRT-III. Two (Ac103 and Ac142), only co-immunoprecipitated with
764 one (Ac103 with Vps24) or two (Ac142 with Vps24 and Vps46) ESCRT-III proteins
765 (Table 3, data not shown). The results suggest that these viral proteins may either
766 interact directly with the ESCRT-III proteins or they may be found in a complex that
767 includes the identified ESCRT-III proteins.

768 To extend the results from co-immunoprecipitation studies, we further examined the
769 possible interactions of ESCRT-III components and viral proteins using a bimolecular
770 fluorescent complementation (BiFC) analysis in living cells. For these studies, Sf9 cells
771 were co-transfected with two plasmids expressing separately the bait and prey proteins,
772 each fused to the N- or C-terminal domain of mCherry (Nm and Cm). Initially, to verify
773 the specificity of the mCherry-based BiFC system in our experimental system, we also
774 selected AcMNPV GP41 and Lef3 as candidate bait and prey proteins. By co-expressing
775 GP41-Nm with either GP41-Cm or Lef3-Cm, we observed mCherry fluorescence
776 complementation in approximately 50% of the cells co-transfected with GP41-Nm and
777 GP41-Cm plasmids. In contrast, fluorescence was not detected in cells co-transfected
778 with GP41-Nm and Lef3-Cm plasmids (data not shown), as expected. Next, we
779 examined interactions among ESCRT-III proteins, or between ESCRT-III proteins and
780 Vps4, by co-expressing Nm and Cm fused proteins in transfected Sf9 cells. Because
781 ESCRT-III proteins are closely associated in a complex and associate with Vps4 during
782 disassembly, BiFC fluorescence was observed in many combinations of ESCRT-III
783 proteins or ESCRT-III proteins and Vps4 (data not shown). The percentages of cells with
784 mCherry fluorescence detected, ranged from 18.7 to 69.8% (data not shown). To
785 examine the interaction of ESCRT-III components and viral proteins, we first added Nm
786 to the C-terminus of ESCRT-III proteins, and Cm to the N-terminus of Ac146 or the C-
787 termini of Ac11, Ac76, Ac78, GP41, Ac93, Ac103, and Ac142. Western blot analysis with
788 anti-HA MAb or an anti-Myc polyclonal antibody showed that all the constructs were
789 expressed in transfected Sf9 cells (Fig. 12A). In the cases of Ac76-Cm and Cm-Ac146,

two bands were detected for each construct, and this has been observed previously (39, 62).

To identify interactions between viral proteins and ESCRT-III proteins, we examined each viral protein (Ac11, Ac76, Ac78, GP41, Ac93, Ac103, Ac142, and Ac146) against each of the ESCRT-III complex proteins (Vps2B, Vps20, Vps24, Snf7, Vps46, or Vps60) in the BiFC analysis (Fig. 12B and C). Three of the viral proteins (Ac76, Ac78, and Ac93) showed strong BiFC with all of the ESCRT-III proteins examined (Fig. 12B and C). Three additional viral proteins (Ac11, GP41, and Ac146) were positive for BiFC with 5 of the 6 ESCRT-III proteins examined, although the specific groups of ESCRT-III proteins that interacted were different. The percentage of fluorescent cells detected in most of these combinations ranged from 5% to 35%, but reached 50% in one combination (Ac76-Cm and Snf7-Nm). One of the viral proteins (Ac103) showed BiFC only with Vps24 (Fig. 12B and C).

While analysis of each ESCRT-III complex protein resulted in BiFC with several viral proteins, Vps2B showed a weaker fluorescence complementation signal than that of other ESCRT-III proteins (Fig. 12B, column Vps2B-Nm). Vps24, on the other hand, had some degree of BiFC with all of the viral proteins examined (Fig. 12B, column Vps24-Nm). Several control experiments were performed to support and confirm the above results. Western blot analysis revealed that all of the constructs were expressed in co-transfected cells (data not shown). Also, similar BiFC fluorescence was observed by performing reciprocal fusions: fusing Nm with viral proteins and Cm with ESCRT-III proteins (data not shown). Taken together, the interactions identified in co-immunoprecipitation assays were consistent with those detected in the complementation

(BiFC) studies. However, few viral protein-ESCRT-III protein interactions that were negative in co-immunoprecipitation analysis were detected by BiFC assays. These included the following combinations: Ac11 and Vps20, Ac78 and Vps2B, Ac142 and Vps20, and Ac146 and Vps20 (Fig. 12, Table 3, data not shown).

Interaction of Vps4 and GP41, Ac93, and Ac103

Vps4 functions in disassembly and recycling of the ESCRT-III complex (7) and prior studies showed that Vps4 is required for efficient egress of AcMNPV budded virions (23). Because we found evidence of interactions between certain viral proteins and ESCRT-III proteins, we also asked whether cellular Vps4 might interact with those viral proteins. To examine this question, we first used an immunoprecipitation assay, HA-tagged viral proteins, as well as Myc-tagged Vps4 and Vps4 mutants, were co-expressed in Sf9 cells and then analyzed by co-immunoprecipitation. Myc-tagged Vps4 and the two dominant-negative forms of Vps4 (K176Q and E231Q) were efficiently co-immunoprecipitated when HA-tagged proteins GP41-HA and Ac93-HA were immunoprecipitated with the anti-HA MAb (Fig. 13B, C). In contrast, other HA-tagged viral proteins (Ac11, Ac76, Ac78, Ac103, Ac142, and Ac146) did not co-immunoprecipitate with Vps4-Myc, K176Q-Myc, or E231Q-Myc (Fig, 13A, D, Table 3). Expression of all proteins was confirmed by Western blot analysis, as described earlier (data not shown). To confirm the immunoprecipitation results, we also used BiFC assay as described earlier, in which we fused the N-terminus of mCherrry (Nm) to the C-terminus of Vps4. In Sf9 cells co-expressing Vps4-Nm in combination with each of the Cm-fused viral proteins described above, we detected fluorescence complementation (BiFC) with viral proteins GP41-Cm, Ac93-Cm, and Ac103-Cm (BiFC was detected in 25%, 35%, and 5% of the cells, respectively) (Fig. 13F,

836 G). Similar levels of fluorescent cells were also observed in cells co-expressing Nm-
837 fused dominant-negative Vps4 proteins (K176Q-Nm and E231Q-Nm). Swapping the Nm
838 and Cm domains between bait and prey proteins had no significant effect on the BiFC
839 fluorescence observed (data not shown). Combined, these results suggest that GP41,
840 Ac93, and possibly Ac103 interact or may be found in complexes with Vps4, and that the
841 interaction does not depend on the ATPase activity of Vps4 since the ATPase deficient
842 DN Vps4 proteins also interacted with these viral proteins.

843 **Interactions among viral proteins**

844 To also examine interactions among these viral proteins, we expressed HA- or Myc-
845 tagged each of these viral proteins (Ac11, Ac76, Ac78, GP41, Ac93, Ac103, Ac142, and
846 Ac146), then co-expressed (homologous or heterologous) combinations of these
847 proteins in Sf9 cells and analyzed the combinations by co-immunoprecipitaion. As shown
848 in Figure S6, each of the viral proteins Ac11, Ac76, Ac78, GP41, Ac93, and Ac146
849 appears to interact with itself and was immunoprecipitated in homologous combinations.
850 For heterologous combinations, co-immunoprecipitation was observed between the
851 following pairs: Ac11-GP41, Ac11-Ac93, Ac76-Ac78, Ac76-Ac93, Ac76-Ac103, Ac78-
852 Ac103, Ac93-Ac103, and Ac103-Ac146 (Table 4, data not shown). The
853 immunoprecipitation results were also confirmed by BiFC analysis. Nm and Cm
854 fragments of mCherry were fused to the N-terminus of Ac146, and to the C-termini of the
855 other viral proteins (Ac11, Ac76, Ac78, GP41, Ac93, Ac103, and Ac142). Expression of
856 all fusion protein constructs was confirmed by Western blot analysis (Fig. 14A; Note:
857 Ac142-Nm and Ac142-Cm are not shown). In cells co-transfected with plasmids
858 expressing the same protein but fused with the Nm and Cm fragments of mCherry, from

20%-45% of the cells showed fluorescence complementation and this was true in all cases (Ac11, Ac76, Ac78, GP41, Ac93, and Ac146) except for Ac103 (Fig. 14B, C), suggesting the self-association of these viral proteins. For heterologous combinations of viral proteins, fluorescence complementation was observed only in cells co-expressing certain combinations (Fig. 14B and C), summarized in Figure 15 (Right panel, center circle). Reciprocal fusions of Nm and Cm with each viral protein did not significantly affect the BiFC detected from the combinations of viral proteins (data not shown). Additionally, no BiFC fluorescence was observed in cells co-expressing Ac142-Nm or Ac142-Cm, with Nm or Cm fused to other viral proteins (data not shown). Thus, we found that the interactions or associations suggested by the co-immunocipitating pairs of viral proteins were confirmed by BiFC in transfected cells co-expressing Nm- and Cm-fused proteins (Fig. 14).

Discussion

The ESCRT machinery is a highly conserved system of protein complexes that mediate membrane budding and scission (2). In addition to its important role in budding and scission of retroviruses and many other RNA and DNA viruses, several studies have demonstrated that the ESCRT system is also sometimes involved in efficient viral entry, assembly, and replication compartment formation (12, 24). Comparatively little is known about the roles of components of the cellular ESCRT pathway in baculovirus infection. In the current study, we found that functional ESCRT-I and ESCRT-III complexes were required for efficient entry and transport of AcMNPV budded virions early in infection. In addition, we found that ESCRT-III but not ESCRT-I played important roles in efficient egress of infectious AcMNPV. These results extend our previous studies using a

dominant-negative Vps4 protein to show that the ESCRT pathway was involved in efficient infection by AcMNPV (23).

Isolation and expression of ESCRT-I and ESCRT-III components of Sf9

Insect genomes encode many of the same ESCRT system components found in yeast and humans. However, the human genome contains a number of gene expansions in the ESCRT-III complex that are not present in insect genomes (40, 41). In insect genomes, gene expansions of the ESCRT-III complex appear to be limited to Vps2 (Vps2A and 2B), as identified in insect species from Phthiraptera, Lepidoptera, and Coleoptera (40). To determine the importance and roles of the cellular ESCRT pathway in AcMNPV infections, we first cloned the ESCRT-I components Tsg101 and Vps28, and ESCRT-III components Vps20, Vps24, Snf7, Vps46, and Vps60. We also isolated an ortholog of Vps2B from Sf9 cells. Amino acid sequence alignment and domain architecture analysis indicated that these ESCRT components of Sf9 are highly conserved with those of other insects and humans. In almost all cases, overexpression of ESCRT-I proteins or DN forms of ESCRT-I or ESCRT-III proteins resulted in cellular localization or aberrant vesicles that were similar to that previously reported in human cells (50-52, 63-65). ESCRT-III proteins contain a basic N-terminus and an acidic C-terminal region (56, 66). Without stimulation, the interaction of C-termini of ESCRT-III subunits with their amino-terminal cores closes the conformation in an autoinhibited monomer state. Removal the intramolecular interaction activates ESCRT-III proteins to assemble as polymers (55, 66). Several prior studies demonstrated that fusion of a bulky tag, such as GFP to the C-terminus of ESCRT-III proteins blocked their autoinhibition and activated ESCRT-III proteins to polymerize. The unregulated assembly of ESCRT-III

complexes resulted in formation of aberrant endosomes (54, 58). We used the same strategy for DN ESCRT-III proteins in the current study and the colocalization of these GFP-tagged ESCRT-III proteins and Vps4 E231Q-mCherry in Sf9 cells suggest that they form a similar aberrant endosome.

ESCRT-I and ESCRT-III are required for efficient entry of AcMNPV

Budded virions of AcMNPV enter host cells via clathrin-dependent endocytosis (28). During entry, membrane fusion mediated by the viral envelope glycoprotein GP64 occurs within the endosome and nucleocapsids are released into the cytosol (25). Nucleocapsids are then transported to the nucleus and through nuclear pore complexes in a process that is mediated by actin polymerization (31, 32). The initial endosomal trafficking of AcMNPV is not well understood although prior studies (23) found that expression of DN Vps4 resulted in an inhibition of both AcMNPV entry and egress. To understand in more detail the role of the ESCRT pathway in viral infection, we examined viral replication and budded virus production using full-length and truncated forms of ESCRT-I, dominant-negative ESCRT-III proteins, and a dsRNA-based RNAi approach. We detected significantly reduced production of infectious AcMNPV budded virions when these forms of ESCRT-I or ESCRT-III proteins were expressed or when ESCRT-I and ESCRT-III proteins were knocked down by RNAi. We used qPCR and mCherry-labeled virions to examine particle entry, and we analyzed early and late reporter gene expression and viral genomic DNA replication to monitor subsequent events in infection. From these studies, we concluded that the reduced production of infectious AcMNPV resulted from the disruption of AcMNPV infection at an early step, prior to early gene expression. Because overexpression or knockdown of ESCRT-I and ESCRT-III proteins

928 resulted in aberrant intracellular compartments, it is likely that entering virions are
929 trafficked through compartments that require functional ESCRT-I or ESCRT-III. In yeast
930 and mammalian cells, endosomal cargo trafficking and formation of MVBs are both
931 dependent on ESCRT-I and ESCRT-III (1, 6, 67).

932 The Tsg101 (UEV domain) is known to interact with so-called viral late domains such
933 as “P(T/S)AP” and genome-wide analysis of AcMNPV revealed that several conserved
934 baculovirus proteins contain a typical late-domain motif. These viral proteins include
935 Ac71 (IAP2), Ac83, and Ac104. Deletion of these genes from the AcMNPV genome has
936 varying effects. Deletion of Ac71 has no effect on infectious virion production (68), but in
937 contrast, deletion of Ac83 or Ac104 each significantly reduces infectious AcMNPV
938 production (69, 70). However, the functional role of the “P(T/S)AP” domain in these viral
939 proteins has not been examined. How the various ESCRT-I constructs interfere with
940 entry/viral infection is unknown but based on prior work we can propose the following
941 possible hypotheses. Because of the presence of the CC domain, Tsg101 constructs
942 dUEV and CC-SB could potentially multimerize with endogenous Tsg101, and all 3 C-
943 terminal forms of Tsg101 (Fig. 1A, dUEV, CC-SB, and SB) might also compete with
944 endogenous Tsg101 for binding with Vps28. Additionally, overexpression of Vps28 might
945 also interfere with the proper assembly of ESCRT-II, which is required for cargo
946 trafficking and ILV formation (6). Previously, it has demonstrated that the CTD domain of
947 Vps28 is not directly involved in ESCRT-I complex assembly, but could function as an
948 adaptor module for the interaction of Vps28 with the ESCRT-III component, Vps20 (53).
949 The effect of Vps28 construct Core (lacking the CTD domain on AcMNPV entry might
950 therefore result from its effect on the assembly of ESCRT-III or recruitment of Vps20.

951 Further studies will be necessary to understand the precise roles of the full-length and
952 truncated forms of Tsg101 and Vps28 on endosomal trafficking and virus entry into
953 insect cells.

954 In yeast, the ESCRT-III complex contains four core components Vps2, Vps20, Vps24,
955 and Snf7 (corresponding mammalians homologs are CHMP2, CHMP6, CHMP3, and
956 CHMP4, respectively) (6, 58). These components assemble in a sequential manner.
957 Vps20 recruits and initiates oligomerization of Snf7, Vps24 caps the oligomer of Snf7
958 and terminates its oligomerization by recruiting Vps2, which in turn recruits Vps4 for
959 disassembly and recycling of ESCRT-III (3, 4, 58). The other two ESCRT-III components
960 Vps46 and Vps60 (CHMP1 and CHMP5 in mammals) are involved in promoting Vps4
961 localization and activation (71-73). Our BiFC results indicated that the ESCRT-III
962 components of Sf9 cells interact with each other, and these components all interact with
963 Vps4, as might be expected. Overexpression of dominant-negative ESCRT-III proteins or
964 Vps4 or RNAi knockdowns of these proteins, likely affect the assembly or disassembly of
965 ESCRT-III, which in turn disrupts endosomal cargo trafficking and ILV formation. Several
966 studies have demonstrated that host ESCRT factors are involved in efficient entry for
967 enveloped viruses such as rhabdoviruses, arenaviruses, flaviviruses, herpesviruses, and
968 bunyaviruses (12, 20-22, 74), as well as the non-enveloped rotavirus (19). Similar to
969 AcMNPV, these viruses enter host cells via receptor-mediated endocytosis and the
970 nucleocapsids are released into the cytoplasm through the limiting membrane of the
971 endosome. The roles of cellular ESCRT complexes or components in the entry of these
972 viruses are not clear and the roles of ESCRT components may differ for different viruses.
973 In the case of VSV where transport during entry has been examined in some detail,

974 interactions may be complex with virions fusing in some cases with the intraluminal
975 vesicles of MVBs, followed by back fusion of ILVs with the limiting membrane of the
976 endosome to release nucleocapsids into cytoplasm (75). It is unclear whether this
977 process occurs in the same manner during entry of BV of AcMNPV, but it is possible that
978 disruption of ESCRT-I or ESCRT-III functions could disrupt successful release of
979 nucleocapsids by interfering with this or other processes in vesicular transport.

980 **Roles of ESCRT-III in efficient egress of AcMNPV**

981 In AcMNPV infected Sf9 cells, substantial quantities of infectious progeny budded
982 viruses are produced at 24 h postinfection (25). Observations from transmission electron
983 microscopy suggest that the progeny nucleocapsids destined to form BV exit the nucleus
984 and transiently obtain an envelope derived from the nuclear membrane (76). In the
985 cytoplasm, the membranes of these vesicles (containing nucleocapsids) are lost by an
986 unknown mechanism (25, 76), and the nucleocapsids are subsequently transported to
987 the plasma membrane where they interact with the plasma membrane and bud to
988 acquire an envelope, forming the budded virions (25). Egress of BV requires kinesin,
989 suggesting that vesicles involved in nucleocapsid egress move along microtubules (77).
990 Because of the importance of ESCRT-I and ESCRT-III components in AcMNPV entry,
991 we could not use the same viral complementation system to study the role of these
992 ESCRT factors in virus egress. Therefore, we transfected insect cells with AcMNPV
993 bacmid DNA encoding and expressing individual ESCRT-I or ESCRT-III protein
994 constructs. The effects of each ESCRT component on virus replication was analyzed at
995 24 h p.t. Using this method for initiating infection, expression of full-length and truncated
996 forms of ESCRT-I components Tsg101 and Vps28, and dominant-negative ESCRT-III

proteins, did not appear to affect or inhibit the early stage of AcMNPV infection as the virus infection progressed into the late phase. In the presence of overexpressed ESCRT-I proteins (full length and truncated forms) we identified no substantial effects on infectious AcMNPV production. However, when dominant-negative ESCRT-III proteins were expressed, we observed reduced production of infectious BV. A substantial reduction in BV production was observed in the presence of either Vps24-GFP, Snf7-GFP, or the control DN Vps4 construct E231Q-GFP (Fig. 8C). A less dramatic reduction was observed when either Vps2B-GFP, Vps46-GFP, or Vps60-GFP was expressed. In one case (overexpression of Vps20-GFP) no apparent reduction in BV production was observed. Similar results were observed from RNAi knockdowns of these ESCRT-III proteins or Vps4 in AcMNPV bacmid DNA transfected cells (Fig. 9C). In total, these data suggest that most of the ESCRT-III proteins are necessary for infectious BV release. Further analysis by confocal microscopy and transmission electronic microscopy suggested that the DN ESCRT-III proteins Vps24-GFP and Snf7-GFP, and Vps4 E231Q-GFP may block nucleocapsid egress from nuclear membrane (Fig. 10, 11). In contrast, an apparently lower level inhibition of nucleocapsids released into the cytoplasm was observed in Vps60-GFP expressing cells. These results suggest that ESCRT-III components Vps24, Snf7, and Vps4 (and possibly Vps2B) may be important for nuclear egress of progeny nucleocapsids.

The role of host ESCRT complex proteins in the context of virus budding has been studied most intensively for retroviruses, particularly HIV-1 (12), which serves as an important paradigm for understanding the roles of the cellular ESCRT pathway in the budding and release of other enveloped viruses (12, 78). Similar to the requirement in

HIV-1 budding, we demonstrated that Snf7 (the homolog of human CHMP4), is critical for AcMNPV BV egress (79). In contrast however, we found that Vps20 (the homolog of human CHMP6), was not necessary for egress of AcMNPV BV. ESCRT protein requirements for egress of AcMNPV differ with those for HIV-1 budding in two other aspects: 1) ESCRT-I components Tsg101 and Vps28 were dispensable for AcMNPV egress, while both are required for HIV-1 budding (80, 81). 2) ESCRT-III proteins Vps24 and Vps60 were both required for efficient AcMNPV egress, but HIV-1 virions are released efficiently in the absence of the human orthologs of Vps24 and Vps60 (CHMP3 and CHMP5) (79). Similar to our observations in AcMNPV egress, Tsg101 is not required for herpes simplex virus (HSV-1) budding, although CHMP3 and CHMP5 are critical for HSV-1 production (82). ESCRT-III is also required for efficient budding of a variety of other viruses, including Epstein-Barr virus and Hepatitis A (12, 18, 83). While the conserved mechanism of membrane fission by the ESCRT-III complex (2) may be utilized by many viruses in the budding process, the different requirements for subunits of ESCRT-III suggest that the mechanism of their recruitment to and assembly at the virus budding sites likely differ between AcMNPV, HIV-1 and other viruses (12).

AcMNPV proteins involved in ESCRT-III recruitment

Several studies have demonstrated that a variety of conserved AcMNPV genes (including Ac11, Ac76, Ac78, Ac80 (GP41), Ac93, Ac103 (p48), Ac142, and Ac146) are essential for production of infectious budded virions. Deletion of these genes individually from the AcMNPV genome does not affect viral DNA replication, but when infections are initiated by transfection with bacmids containing knockouts in most of these genes, progeny nucleocapsids are not efficiently released from the nucleus (34-39, 59, 60).

1043 Western blot analysis indicated that Ac76, Ac78, and Ac93 are all present on the
1044 envelope of BV and ODV (35, 37, 62). Ac142 and Ac146 are associated with the
1045 nucleocapsid of BV (38, 39), and Ac80 (GP41) is an ODV tegument protein (25). To
1046 determine whether these viral proteins may interact with ESCRT-III/Vps4, we examined
1047 combinations of viral and host proteins in Co-IP and BiFC assays. We found that these
1048 viral proteins interacted or were associated with each other and with ESCRT-III subunits
1049 and Vps4 in a complex manner (Fig. 15). Intriguingly, Ac76, Ac78, and Ac93 (viral
1050 proteins found on both BV and ODV envelopes) appear to interact with all ESCRT-III
1051 proteins, highlighting the potentially central role of these viral proteins in either recruiting
1052 or functionally interacting with ESCRT-III components. Ac11, Ac146, and GP41 also
1053 interacted broadly, with 5 of the 6 ESCRT-III proteins, suggesting that they may also be
1054 involved in recruiting or in functional interactions in the ESCRT-III fission machine. For
1055 viral proteins Ac103, and Ac142, we identified interactions with only one (Ac103) or a few
1056 (Ac142) ESCRT-III proteins, although this does not imply that they may not play an
1057 important role. Our data suggested that three viral proteins (Ac93, Ac103, and GP41)
1058 interact directly or indirectly with Vps4, and these viral proteins could play a role in
1059 recruiting or activating Vps4. These three viral proteins also interacted with the modified
1060 (ATPase-defective) form of Vps4, suggesting that their interactions did not depend on
1061 Vps4 ATPase activity.

1062 In yeast and mammals, Snf7 (CHMP4) is the most abundant ESCRT-III component
1063 and it plays central roles in ESCRT-III polymer formation and membrane fission (84).
1064 The detection of interactions between multiple AcMNPV proteins and Vps20 or Snf7 may
1065 indicate redundancies in recruiting Snf7, i.e. via viral proteins interacting with Snf7 or

viral proteins interacting with Vps20 which recruits Snf7. These possibly redundant interactions might explain why dominant-negative Vps20 or RNAi knockdown of this protein did not block production of infectious BV.

In addition to their roles in egress of progeny nucleocapsids from the nuclear membrane, viral proteins Ac11, Ac76, Ac93, Ac103, and Ac142 are also required for envelopment of nucleocapsids in the nucleus to form ODV (34, 36-38, 60). Deletion of Ac76 or Ac93 resulted in reduced formation of the virus-induced intranuclear microvesicles (34, 37), which are derived from the inner nuclear membrane and are the source for ODV envelopes (26, 27, 76). We found that in addition to their roles in ODV formation, they also have a complex web of interactions with host ESCRT-III proteins and Vps4. Viral genes Ac76, Ac78, GP41, Ac93, Ac103, Ac142 are core baculovirus genes that are present in most or all sequenced baculovirus genomes (Note: Ac76 was not identified in the dipteran virus genome but is present in all other sequenced baculovirus genomes.) (25, 85). Because these genes are conserved across baculovirus genomes, and serve critical roles in BV egress and ODV formation, this suggests a long and important evolutionary association with cellular pathways critical for production of BV and ODV.

Based on our observations and prior studies of these viral proteins, we developed a hypothetical model of the coordinated action of viral proteins and ESCRT-III/Vps4 in efficient budding of progeny nucleocapsids from the nuclear membrane (Fig. 13). In this model, we hypothesize that the viral core protein Ac76 (which is one of the most highly expressed late genes) accumulates in the inner nuclear membrane (62, 86) to form a shell and initiates the nuclear membrane protrusion. In this process, the interaction of

viral core proteins Ac78 and Ac93 with Ac76 might also contribute. Another viral core protein, Ac103, bridges the Ac76-Ac78-Ac93 complex and Ac146, which is present in the nucleocapsid. Through these interactions, the progeny nucleocapsid might be directed to the budding region on the nuclear membrane (Fig. 16A). The core viral capsid protein Ac142 might also be involved in targeting the nucleocapsid. In addition to initiating nuclear membrane remodeling, the complex Ac76-Ac78-Ac93 may interact with Ac11 and GP41 to recruit the core components of ESCRT-III (which include Vps2, Vps20, Vps24, and Snf7). These ESCRT-III proteins may then form a complex to build the filament of Snf7 that constricts the nuclear membrane (Fig. 16B). After releasing the vesicle containing the nucleocapsid from the nuclear membrane, the viral protein complex would further recruit Vps4 and the ESCRT-III proteins Vps46 and Vps60, which are required for activating of Vps4. The disassembly and recycling of the ESCRT-III complex would then be catalyzed by the Vps4 complex (Fig. 16C). While highly speculative, this hypothetical model for nucleocapsid trafficking is based on prior and current results, and provides a framework for future experimental analysis. Validation of this or other models may require high-resolution microscopy to localize viral and host protein complexes and cellular compartments associated with virus entry and egress.

Acknowledgements

The authors thank Taro Ohkawa and Matthew Welch for the kind gift of virus 3mC. This work was supported by grants from the National Natural Science Foundation of China (NSFC, No. 31672082, 31272088,) and National Key R&D Program of China (2017YFC1200605) to Z.L. and grants from the National Science Foundation (NSF IOS-

1111 1354421) and United States Department of Agriculture (USDA, 2015-67013-23281) to
1112 G.W.B.

References

1. **Henne WM, Buchkovich NJ, Emr SD.** 2011. The ESCRT pathway. Dev Cell **21:**77-91.
2. **Hurley JH.** 2015. ESCRTs are everywhere. EMBO J **34:**2398-2407.
3. **Guizetti J, Gerlich DW.** 2012. ESCRT-III polymers in membrane neck constriction. Trends Cell Biol **22:**133-140.
4. **Henne WM, Stenmark H, Emr SD.** 2013. Molecular mechanisms of the membrane sculpting ESCRT pathway. Cold Spring Harb Perspect Biol **5**.
5. **Webster BM, Colombi P, Jager J, Lusk CP.** 2014. Surveillance of nuclear pore complex assembly by ESCRT-III/Vps4. Cell **159:**388-401.
6. **McCullough J, Colf LA, Sundquist WI.** 2013. Membrane fission reactions of the mammalian ESCRT pathway. Annu Rev Biochem **82:**663-692.
7. **Yang B, Stjepanovic G, Shen Q, Martin A, Hurley JH.** 2015. Vps4 disassembles an ESCRT-III filament by global unfolding and processive translocation. Nat Struct Mol Biol **22:**492-498.
8. **Norgan AP, Davies BA, Azmi IF, Schroeder AS, Payne JA, Lynch GM, Xu Z, Katzmann DJ.** 2013. Relief of autoinhibition enhances Vta1 activation of Vps4 via the Vps4 stimulatory element. J Biol Chem **288:**26147-26156.
9. **Wollert T, Hurley JH.** 2010. Molecular mechanism of multivesicular body biogenesis by ESCRT complexes. Nature **464:**864-869.
10. **Jimenez AJ, Maiuri P, Lafaurie-Janvore J, Divoux S, Piel M, Perez F.** 2014. ESCRT machinery is required for plasma membrane repair. Science **343:**1247136.
11. **Vietri M, Schink KO, Campsteijn C, Wegner CS, Schultz SW, Christ L, Thoresen SB, Brech A, Raiborg C, Stenmark H.** 2015. Spastin and ESCRT-III coordinate mitotic spindle disassembly and nuclear envelope sealing. Nature **522:**231-235.
12. **Votteler J, Sundquist WI.** 2013. Virus budding and the ESCRT pathway. Cell Host Microbe **14:**232-241.
13. **Nakayama K.** 2016. Regulation of cytokinesis by membrane trafficking involving small GTPases and the ESCRT machinery. Crit Rev Biochem Mol Biol **51:**1-6.

14. **Prescher J, Baumgartel V, Ivanchenko S, Torrano AA, Brauchle C, Muller B, Lamb DC.** 2015. Super-resolution imaging of ESCRT-proteins at HIV-1 assembly sites. PLoS Pathog **11:**e1004677.

15. **Van Engelenburg SB, Shtengel G, Sengupta P, Waki K, Jarnik M, Ablan SD, Freed EO, Hess HF, Lippincott-Schwartz J.** 2014. Distribution of ESCRT machinery at HIV assembly sites reveals virus scaffolding of ESCRT subunits. Science **343:**653-656.

16. **Bleck M, Itano MS, Johnson DS, Thomas VK, North AJ, Bieniasz PD, Simon SM.** 2014. Temporal and spatial organization of ESCRT protein recruitment during HIV-1 budding. Proc Natl Acad Sci U S A **111:**12211-12216.

17. **Wirblich C, Bhattacharya B, Roy P.** 2006. Nonstructural protein 3 of bluetongue virus assists virus release by recruiting ESCRT-I protein Tsg101. J Virol **80:**460-473.

18. **Feng Z, Hensley L, McKnight KL, Hu F, Madden V, Ping L, Jeong SH, Walker C, Lanford RE, Lemon SM.** 2013. A pathogenic picornavirus acquires an envelope by hijacking cellular membranes. Nature **496:**367-371.

19. **Silva-Ayala D, Lopez T, Gutierrez M, Perrimon N, Lopez S, Arias CF.** 2013. Genome-wide RNAi screen reveals a role for the ESCRT complex in rotavirus cell entry. Proc Natl Acad Sci U S A **110:**10270-10275.

20. **Shtanko O, Nikitina RA, Altuntas CZ, Chepurnov AA, Davey RA.** 2014. Crimean-Congo hemorrhagic fever virus entry into host cells occurs through the multivesicular body and requires ESCRT regulators. PLoS Pathog **10:**e1004390.

21. **Veettil MV, Kumar B, Ansari MA, Dutta D, Iqbal J, Gjyshi O, Bottero V, Chandran B.** 2016. ESCRT-0 component Hrs promotes macropinocytosis of Kaposi's sarcoma-associated herpesvirus in human dermal microvascular endothelial cells. J Virol **90:**3860-3872.

22. **Pasqual G, Rojek JM, Masin M, Chatton JY, Kunz S.** 2011. Old world arenaviruses enter the host cell via the multivesicular body and depend on the endosomal sorting complex required for transport. PLoS Pathog **7:**e1002232.

23. **Li Z, Blissard GW.** 2012. Cellular VPS4 is required for efficient entry and egress of budded virions of Autographa californica multiple nucleopolyhedrovirus. J Virol **86:**459-472.

24. **Diaz A, Zhang J, Ollwerther A, Wang X, Ahlquist P.** 2015. Host ESCRT proteins are required for bromovirus RNA replication compartment assembly and function. PLoS Pathog **11:**e1004742.

25. **Rohrmann G.** 2013. Baculovirus Molecular Biology: Third Edition [Internet]. National Center for Biotechnology Information (US), Bethesda (MD).

26. **Shi Y, Li K, Tang P, Li Y, Zhou Q, Yang K, Zhang Q.** 2015. Three-dimensional visualization of the Autographa californica multiple nucleopolyhedrovirus occlusion-derived virion envelopment process gives new clues as to its mechanism. Virology **476:**298-303.

27. **Braunagel SC, Elton DM, Ma H, Summers MD.** 1996. Identification and analysis of an Autographa californica nuclear polyhedrosis virus structural protein of the occlusion-derived virus envelope: ODV-E56. Virology **217:**97-110.

28. **Long G, Pan X, Kormelink R, Vlak JM.** 2006. Functional entry of baculovirus into insect and mammalian cells is dependent on clathrin-mediated endocytosis. J Virol **80:**8830-8833.

29. **Blissard GW, Wenz JR.** 1992. Baculovirus gp64 envelope glycoprotein is sufficient to mediate pH-dependent membrane fusion. J Virol **66:**6829-6835.

30. **Zhou J, Blissard GW.** 2008. Identification of a GP64 subdomain involved in receptor binding by budded virions of the baculovirus Autographica californica multicapsid nucleopolyhedrovirus. J Virol **82:**4449-4460.

31. **Ohkawa T, Volkman LE, Welch MD.** 2010. Actin-based motility drives baculovirus transit to the nucleus and cell surface. J Cell Biol **190:**187-195.

32. **Au S, Pante N.** 2012. Nuclear transport of baculovirus: revealing the nuclear pore complex passage. J Struct Biol **177:**90-98.

33. **Oomens AG, Blissard GW.** 1999. Requirement for GP64 to drive efficient budding of Autographa californica multicapsid nucleopolyhedrovirus. Virology **254:**297-314.

34. **Hu Z, Yuan M, Wu W, Liu C, Yang K, Pang Y.** 2010. Autographa californica multiple nucleopolyhedrovirus ac76 is involved in intranuclear microvesicle formation. J Virol **84:**7437-7447.

35. **Tao XY, Choi JY, Kim WJ, Lee JH, Liu Q, Kim SE, An SB, Lee SH, Woo SD, Jin BR, Je YH.** 2013. The Autographa californica multiple nucleopolyhedrovirus ORF78 is essential for budded virus production and general occlusion body formation. J Virol **87:**8441-8450.

36. **Yuan M, Wu W, Liu C, Wang Y, Hu Z, Yang K, Pang Y.** 2008. A highly conserved baculovirus gene p48 (ac103) is essential for BV production and ODV envelopment. Virology **379:**87-96.

37. **Yuan M, Huang Z, Wei D, Hu Z, Yang K, Pang Y.** 2011. Identification of Autographa californica nucleopolyhedrovirus ac93 as a core gene and its requirement for intranuclear microvesicle formation and nuclear egress of nucleocapsids. J Virol **85:**11664-11674.

38. **McCarthy CB, Dai X, Donly C, Theilmann DA.** 2008. Autographa californica multiple nucleopolyhedrovirus ac142, a core gene that is essential for BV production and ODV envelopment. Virology **372:**325-339.

39. **Dickison VL, Willis LG, Sokal NR, Theilmann DA.** 2012. Deletion of AcMNPV ac146 eliminates the production of budded virus. Virology **431:**29-39.

40. **Li Z, Blissard G.** 2015. The vacuolar protein sorting genes in insects: A comparative genome view. Insect Biochem Mol Biol **62:**211-225.

41. **Chen YR, Zhong S, Fei Z, Gao S, Zhang S, Li Z, Wang P, Blissard GW.** 2014. Transcriptome responses of the host Trichoplusia ni to infection by the baculovirus Autographa californica multiple nucleopolyhedrovirus. J Virol **88:**13781-13797.

42. **Plonsky I, Cho MS, Oomens AG, Blissard G, Zimmerberg J.** 1999. An analysis of the role of the target membrane on the Gp64-induced fusion pore. Virology **253:**65-76.

43. **Negre V, Hotelier T, Volkoff AN, Gimenez S, Cousserans F, Mita K, Sabau X, Rocher J, Lopez-Ferber M, d'Alencon E, Audant P, Sabourault C,**

Bidegainberry V, Hilliou F, Fournier P. 2006. SPODOBASE: an EST database for the lepidopteran crop pest Spodoptera. BMC Bioinformatics **7:**322.

44. **Guo Y, Yue Q, Gao J, Wang Z, Chen YR, Blissard GW, Liu TX, Li Z.** 2017. Roles of cellular NSF protein in entry and nuclear egress of budded virions of Autographa californica multiple nucleopolyhedrovirus. J Virol **91:** doi: 10.1128/JVI.01111-17.

45. **Fan JY, Cui ZQ, Wei HP, Zhang ZP, Zhou YF, Wang YP, Zhang XE.** 2008. Split mCherry as a new red bimolecular fluorescence complementation system for visualizing protein-protein interactions in living cells. Biochem Biophys Res Commun **367:**47-53.

46. **Luckow VA, Lee SC, Barry GF, Olins PO.** 1993. Efficient generation of infectious recombinant baculoviruses by site-specific transposon-mediated insertion of foreign genes into a baculovirus genome propagated in Escherichia coli. J Virol **67:**4566-4579.

47. **Li Z, Blissard GW.** 2008. Functional analysis of the transmembrane (TM) domain of the Autographa californica multicapsid nucleopolyhedrovirus GP64 protein: substitution of heterologous TM domains. J Virol **82:**3329-3341.

48. **Deng Z, Huang Z, Yuan M, Yang K, Pang Y.** 2014. Baculovirus induces host cell aggregation via a Rho/Rok-dependent mechanism. J Gen Virol **95:**2310-2320.

49. **Yu Q, Blissard GW, Liu TX, Li Z.** 2016. Autographa californica multiple nucleopolyhedrovirus GP64 protein: Analysis of domain I and V amino acid interactions and membrane fusion activity. Virology **488:**259-270.

50. **Goila-Gaur R, Demirov DG, Orenstein JM, Ono A, Freed EO.** 2003. Defects in human immunodeficiency virus budding and endosomal sorting induced by TSG101 overexpression. J Virol **77:**6507-6519.

51. **Martin-Serrano J, Zang T, Bieniasz PD.** 2003. Role of ESCRT-I in retroviral budding. J Virol **77:**4794-4804.

52. **Johnson MC, Spidel JL, Ako-Adjei D, Wills JW, Vogt VM.** 2005. The C-terminal half of TSG101 blocks Rous sarcoma virus budding and sequesters Gag into unique nonendosomal structures. J Virol **79:**3775-3786.

53. **Pineda-Molina E, Belrhali H, Piefer AJ, Akula I, Bates P, Weissenhorn W.** 2006. The crystal structure of the C-terminal domain of Vps28 reveals a conserved surface required for Vps20 recruitment. Traffic **7:**1007-1016.

54. **Zamborlini A, Usami Y, Radoshitzky SR, Popova E, Palu G, Gottlinger H.** 2006. Release of autoinhibition converts ESCRT-III components into potent inhibitors of HIV-1 budding. Proc Natl Acad Sci U S A **103:**19140-19145.

55. **Bajorek M, Schubert HL, McCullough J, Langelier C, Eckert DM, Stubblefield WM, Uter NT, Myszka DG, Hill CP, Sundquist WI.** 2009. Structural basis for ESCRT-III protein autoinhibition. Nat Struct Mol Biol **16:**754-762.

56. **Muziol T, Pineda-Molina E, Ravelli RB, Zamborlini A, Usami Y, Gottlinger H, Weissenhorn W.** 2006. Structural basis for budding by the ESCRT-III factor CHMP3. Dev Cell **10:**821-830.

57. **Strack B, Calistri A, Craig S, Popova E, Gottlinger HG.** 2003. AIP1/ALIX is a binding partner for HIV-1 p6 and EIAV p9 functioning in virus budding. Cell **114:**689-699.

58. **Teis D, Saksena S, Emr SD.** 2008. Ordered assembly of the ESCRT-III complex on endosomes is required to sequester cargo during MVB formation. Dev Cell **15:**578-589.

59. **Olszewski J, Miller LK.** 1997. A role for baculovirus GP41 in budded virus production. Virology **233:**292-301.

60. **Tao XY, Choi JY, Kim WJ, An SB, Liu Q, Kim SE, Lee SH, Kim JH, Woo SD, Jin BR, Je YH.** 2015. Autographa californica multiple nucleopolyhedrovirus ORF11 is essential for budded-virus production and occlusion-derived-virus envelopment. J Virol **89:**373-383.

61. **Peng K, Wu M, Deng F, Song J, Dong C, Wang H, Hu Z.** 2010. Identification of protein-protein interactions of the occlusion-derived virus-associated proteins of Helicoverpa armigera nucleopolyhedrovirus. J Gen Virol **91:**659-670.

62. **Wei D, Wang Y, Zhang X, Hu Z, Yuan M, Yang K.** 2014. Autographa californica nucleopolyhedrovirus Ac76: a dimeric type II integral membrane protein that contains an inner nuclear membrane-sorting motif. J Virol **88:**1090-1103.

63. **Kostelansky MS, Schluter C, Tam YY, Lee S, Ghirlando R, Beach B, Conibear E, Hurley JH.** 2007. Molecular architecture and functional model of the complete yeast ESCRT-I heterotetramer. Cell **129:**485-498.

64. **Lee HH, Elia N, Ghirlando R, Lippincott-Schwartz J, Hurley JH.** 2008. Midbody targeting of the ESCRT machinery by a noncanonical coiled coil in CEP55. Science **322:**576-580.

65. **Gill DJ, Teo H, Sun J, Perisic O, Veprintsev DB, Emr SD, Williams RL.** 2007. Structural insight into the ESCRT-I/-II link and its role in MVB trafficking. EMBO J **26:**600-612.

66. **Lata S, Roessle M, Solomons J, Jamin M, Gottlinger HG, Svergun DI, Weissenhorn W.** 2008. Structural basis for autoinhibition of ESCRT-III CHMP3. J Mol Biol **378:**818-827.

67. **Schuh AL, Audhya A.** 2014. The ESCRT machinery: from the plasma membrane to endosomes and back again. Crit Rev Biochem Mol Biol **49:**242-261.

68. **Griffiths CM, Barnett AL, Ayres MD, Windass J, King LA, Possee RD.** 1999. In vitro host range of Autographa californica nucleopolyhedrovirus recombinants lacking functional p35, iap1 or iap2. J Gen Virol **80 (Pt 4):**1055-1066.

69. **Zhu S, Wang W, Wang Y, Yuan M, Yang K.** 2013. The baculovirus core gene ac83 is required for nucleocapsid assembly and per os infectivity of Autographa californica nucleopolyhedrovirus. J Virol **87:**10573-10586.

70. **Marek M, van Oers MM, Devaraj FF, Vlak JM, Merten OW.** 2011. Engineering of baculovirus vectors for the manufacture of virion-free biopharmaceuticals. Biotech Bioeng **108:**1056-1067.

71. **Lottridge JM, Flannery AR, Vincelli JL, Stevens TH.** 2006. Vta1p and Vps46p regulate the membrane association and ATPase activity of Vps4p at the yeast multivesicular body. Proc Natl Acad Sci U S A **103:**6202-6207.

72. **Shim JH, Xiao C, Hayden MS, Lee KY, Trombetta ES, Pypaert M, Nara A, Yoshimori T, Wilm B, Erdjument-Bromage H, Tempst P, Hogan BL, Mellman I, Ghosh S.** 2006. CHMP5 is essential for late endosome function and down-regulation of receptor signaling during mouse embryogenesis. J Cell Biol **172:**1045-1056.

73. **Yang Z, Vild C, Ju J, Zhang X, Liu J, Shen J, Zhao B, Lan W, Gong F, Liu M, Cao C, Xu Z.** 2012. Structural basis of molecular recognition between ESCRT-III-like protein Vps60 and AAA-ATPase regulator Vta1 in the multivesicular body pathway. J Biol Chem **287:**43899-43908.

74. **Luyet PP, Falguieres T, Pons V, Pattnaik AK, Gruenberg J.** 2008. The ESCRT-I subunit TSG101 controls endosome-to-cytosol release of viral RNA. Traffic **9:**2279-2290.

75. **Le Blanc I, Luyet PP, Pons V, Ferguson C, Emans N, Petiot A, Mayran N, Demaurex N, Faure J, Sadoul R, Parton RG, Gruenberg J.** 2005. Endosome-to-cytosol transport of viral nucleocapsids. Nat Cell Biol **7:**653-664.

76. **Fraser M.** 1986. Ultrastructural observations of virion maturation in Autographa californica nuclear polyhedrosis virus infected *Spodoptera frugiperda* cell cultures. J Ultrastruct Mol Struct Res **95:**189-195.

77. **Biswas S, Blissard GW, Theilmann DA.** 2016. Trichoplusia ni kinesin-1 associates with AcMNPV nucleocapsid proteins and is required for the production of budded virus. J Virol **90:** 3480-3495.

78. **Martin-Serrano J, Neil SJ.** 2011. Host factors involved in retroviral budding and release. Nat Rev Microbiol **9:**519-531.

79. **Morita E, Sandrin V, McCullough J, Katsuyama A, Baci Hamilton I, Sundquist WI.** 2011. ESCRT-III protein requirements for HIV-1 budding. Cell Host Microbe **9:**235-242.

80. **Demirov DG, Ono A, Orenstein JM, Freed EO.** 2002. Overexpression of the N-terminal domain of TSG101 inhibits HIV-1 budding by blocking late domain function. Proc Natl Acad Sci U S A **99:**955-960.

81. **Morita E, Sundquist WI.** 2004. Retrovirus budding. Annu Rev Cell Dev Biol **20:**395-425.

82. **Pawliczek T, Crump CM.** 2009. Herpes simplex virus type 1 production requires a functional ESCRT-III complex but is independent of TSG101 and ALIX expression. J Virol **83:**11254-11264.

83. **Lee CP, Liu PT, Kung HN, Su MT, Chua HH, Chang YH, Chang CW, Tsai CH, Liu FT, Chen MR.** 2012. The ESCRT machinery is recruited by the viral BFRF1

protein to the nucleus-associated membrane for the maturation of Epstein-Barr Virus. PLoS Pathog **8:**e1002904.

84. **Chiaruttini N, Redondo-Morata L, Colom A, Humbert F, Lenz M, Scheuring S, Roux A.** 2015. Relaxation of loaded ESCRT-III spiral springs drives membrane deformation. Cell **163:**866-879.

85. **Afonso CL, Tulman ER, Lu Z, Balinsky CA, Moser BA, Becnel JJ, Rock DL, Kutish GF.** 2001. Genome sequence of a baculovirus pathogenic for Culex nigripalpus. J Virol **75:**11157-11165.

86. **Chen YR, Zhong S, Fei Z, Hashimoto Y, Xiang JZ, Zhang S, Blissard GW.** 2013. The transcriptome of the baculovirus Autographa californica multiple nucleopolyhedrovirus in Trichoplusia ni cells. J Virol **87:**6391-6405.

Figure Legends

Figure 1

Construction and transient expression of GFP-tagged wild-type or truncated forms of ESCRT-I components Tsg101 and Vps28. (A) Schematic representation of the domain organization of WT Tsg101 and Vps28, and truncated forms of each. Numbers on the right denote the amino acid sequence length of each construct. Abbreviations: CC, coiled-coil; CTD, C-terminal four helix bundle domain; dUEV, deletion of UEV domain; PRD, proline-rich domain; SB, steadiness box; UEV, ubiquitin-enzyme variant domain. (B, C) Expression of GFP-tagged WT or truncated forms of Tsg101 and Vps28 in transfected Sf9 cells. (B) The expression of GFP-tagged Tsg101 and Vps28 constructs was analyzed by Western blotting using a GFP-specific polyclonal antibody, gels spliced for labeling purposes. (C) The cellular distribution of GFP-tagged Tsg101 and Vps28 constructs was visualized by epifluorescence microscopy (Epi, left panels) and confocal microscopy (Confocal, right panels). Phase-contrast images on the left side illustrate the presence of vesicles induced by Vps28 construct Core which lacks the CTD domain. (D) Colocalization of GFP-tagged Tsg101 and Vps28 constructs with mCherry-tagged Vps4 mutant E231Q in co-transfected Sf9 cells. Cell boundaries were traced with circled dash lines. Scale bar, 10 μm.

Figure 2

Transient expression of GFP-tagged ESCRT-III components in Sf9 cells. (A) Schematic representation of the ESCRT-III components cloned from Sf9 cells. The predicted Snf7 domain of each component is shown as a black box, and the start and end amino acids of Snf7 domains in individual components are indicated. The amino

acid sequence length for each protein is indicated on the right. (B, C) Expression of GFP-tagged ESCRT-III proteins in transfected Sf9 cells. (B) The expression of GFP-tagged ESCRT-III proteins was analyzed by Western blotting using a GFP-specific polyclonal antibody, gels spliced for labeling purposes. (C) The cellular distribution of GFP-tagged ESCRT-III proteins was visualized by epifluorescence microscopy (Epi: left panels) and confocal microscopy (Confocal: right panels). The presence of vesicles induced by dominant-negative ESCRT-III constructs can be observed in phase-contrast images on the left. (D) Colocalization of GFP-tagged ESCRT-III proteins with mCherry-tagged Vps4 mutant E231Q in co-transfected Sf9 cells. Cell boundaries were traced with circled dash lines. Scale bar, 10 μm.

Figure 3

Transient expression of GFP-tagged ESCRT-I and ESCRT-III proteins significantly inhibit the production of infectious AcMNPV in a viral complementation assay. (A) Schematic representation of the viral complementation assay. a. In cells transfected with a *gp64* knockout AcMNPV bacmid, virus budding is defective. When the *gp64* knockout bacmid DNA is transfected into $Sf9^{Op1D}$ cells that stably express OpMNPV GP64, virus budding and infectivity are complemented by OpMNPV GP64. b. Sf9 cells are co-transfected with two plasmids separately expressing AcMNPV GP64 (pBieGP64) and GFP or a GFP-tagged ESCRT protein. At 16 h p.t., the cells are infected with a *gp64* knockout AcMNPV virus that was produced in $Sf9^{Op1D}$ cells and containing the OpMNPV GP64 protein on its surface. Because all cells do not become transfected, the *gp64* knockout AcMNPV can only bud and propagate in cells that are productively transfected, expressing both GFP or the GFP-tagged ESCRT

protein and AcMNPV GP64, which complements the *gp64* knockout. In non-transfected cells, the *gp64* knockout AcMNPV virus can enter the cells but budding of progeny virions is defective. (B, C) Sf9 cells were co-transfected with a plasmid expressing GP64 together with a plasmid encoding GFP-tagged ESCRT-I and ESCRT-III proteins, E231Q-GFP or GFP. At 16 h p.t., the cells were infected with a *gp64* knockout AcMNPV at an MOI of 1 or 5. At 24 h p.i., the titers of progeny viruses from cell culture medium were determined by $TCID_{50}$ assay on a GP64 complementing cell line ($Sf9^{OP1D}$). Error bars indicate the standard deviation from the mean of triplicate samples. (D) The expression of GP64 and GFP-tagged ESCRT-I and ESCRT-III proteins in co-transfected and infected cells were analyzed by Western blotting using anti-GP64 MAb (AcV5) and an anti-GFP polyclonal antibody, gels spliced for labeling purposes. *, $p<0.005$ (by unpaired *t* test).

Figure 4

RNAi knockdown of ESCRT-I or ESCRT-III proteins inhibit production of infectious AcMNPV. (A) Sf9 cells were transfected with a plasmid expressing HA- or c-Myc-tagged ESCRT-I, ESCRT-III proteins or Vps4, or co-transfected with a plasmid expressing individual HA- or c-Myc-tagged ESCRT protein and a dsRNA specific an ESCRT gene or GFP. At 48 h p.t., the transfected cells were collected and expression of the HA- or c-Myc-tagged ESCRT protein was detected by Western blot analysis with an anti-HA monoclonal antibody or an anti-Myc polyclonal antibody. Actin was detected (using anti-β-actin) as a loading control. (B) Sf9 cells were mock transfected or transfected with the dsRNA specific for GFP or for an individual ESCRT gene. At 48 h p.t., the transfected

1434 cells were infected with control AcMNPV. At 24 h p.i., the cell culture supernatants were
1435 collected and virus titers were determined by $TCID_{50}$. **, p<0.0005 (by unpaired *t* test).

1436 **Figure 5**

1437 **Effects of overexpression of GFP-tagged ESCRT-I and ESCRT-III proteins on**
1438 **early stages of AcMNPV replication.** Sf9 cells were co-transfected with two plasmids
1439 separately expressing a) GP64 and b) one of the GFP-tagged ESCRT-I or ESCRT-III
1440 proteins, E231Q-GFP or GFP. At 16 h p.t., the cells were infected with a *gp64* knockout
1441 virus LacZGUS-*gp64*^{ko} (MOI=5). At 6 h p.i., the infected cells were collected and the
1442 early reporter (beta-galactosidase) activity was measured using CPRG as the substrate
1443 (A, B). At 24 h p.i. the parallel transfected and infected cells were lysed and the late
1444 reporter (GUS) activity was measured (C, D) and viral genomic DNA replication
1445 efficiency was evaluated by real-time PCR (E, F). Error bars indicate standard deviation
1446 of the mean from three replicates. *, p<0.005; **, p<0.0005; ***, p<0.00005 (by unpaired
1447 *t* test).

1448 **Figure 6**

1449 **Analysis of the effects of overexpression of GFP-tagged ESCRT-I and ESCRT-III**
1450 **proteins on entry of AcMNPV.** Sf9 cells were co-transfected with two plasmids
1451 separately expressing a) GP64 and b) one of the GFP-tagged ESCRT-I or ESCRT-III
1452 proteins, E231Q-GFP, or GFP. At 16 h p.t., cells were infected with pre-chilled control
1453 AcMNPV or an mCherry-labeled AcMNPV virus (3mC) (MOI=10 $TCID_{50}$) at 4° for 1 h,
1454 then the cells were incubated at 27° for 90 min. The control AcMNPV infected cells were
1455 lysed and the internalized viral genomic DNAs were determined by real-time PCR (A, B).
1456 The 3mC virus infected cells were fixed and analyzed by confocal microscopy (C). Cell

1457 boundaries were traced with circled dash lines. Scale bar, 10 μm. *, p<0.005; **,
1458 p<0.0005 (by unpaired *t* test).

1459 **Figure 7**

1460 **Analysis of the effects of RNAi knockdowns targeting specific ESCRT-I and**
1461 **ESCRT-III genes on entry of AcMNPV.** Sf9 cells were mock transfected or transfected
1462 with the dsRNA targeting an individual ESCRT-I or ESCRT-III gene, Vps4 or GFP. At 48
1463 h p.t., cells were infected with pre-chilled control AcMNPV or an mCherry-labeled
1464 AcMNPV virus (3mC) (MOI=10) at 4° for 1 h, then the cells were incubated at 27° for 90
1465 min. The control AcMNPV-infected cells were lysed and the internalized viral genomic
1466 DNAs were determined by quantitative real-time PCR (A). The 3mC virus infected cells
1467 were fixed and analyzed by confocal microscopy (B). Cell boundaries were traced with
1468 dashed lines. Scale bar, 10 μm. Error bars represent standard deviations from the mean
1469 of three replicates. **, p<0.0005 (by unpaired *t* test).

1470 **Figure 8**

1471 **Infectious BV production in the presence of GFP-tagged ESCRT-I and ESCRT-III**
1472 **proteins expressed from AcMNPV bacmids.** Sf9 cells were transfected with AcMNPV
1473 bacmids expressing either a) one of the GFP-tagged ESCRT-I or ESCRT-III proteins, b)
1474 E231Q-GFP, or c) GFP. At 24 h p.t., the percentage of GFP-expressing cells was
1475 determined for each treatment and percentages are shown below each panel as an
1476 estimate of transfection efficiency (A). A parallel group of transfected cells were also
1477 lysed at 24 h p.t. and GUS activity (expressed from late GUS reporter gene, driven by a
1478 *p6.9* late promoter in each bacmid) was determined (B). The production of infectious BV
1479 from each treatment was determined by $TCID_{50}$ assay of the cell supernatant (C). Error

bars represent standard deviations from the mean of three replicates. *, p<0.005; ***, p<0.00005 (by unpaired *t* test).

Figure 9

Analysis of the effects of RNAi knockdowns targeting specific ESCRT-I and ESCRT-III genes on infectious AcMNPV BV release. Sf9 cells were mock transfected or transfected with the dsRNA targeting an individual ESCRT-I or ESCRT-III gene, or the control GFP gene. At 48 h p.t., the cells were transfected again with control AcMNPV bacmid DNA (AcMNPV-LacZGUS). After transfection with the viral bacmid DNA for 24 h, the transfected cells were lysed and beta-Gal and GUS activities (separately expressed from early LacZ and late GUS reporter genes, driven by an *ie2* early promoter and a *p6.9* late promoter respectively in each bacmid) was determined (A, B). The production of infectious BV from each treatment was determined by $TCID_{50}$ assay of the cell supernatant (C). Error bars represent standard deviations from the mean of three replicates. *, p<0.005; ***, p<0.00005 (by unpaired *t* test).

Figure 10

Dominant-negative ESCRT-III and Vps4 proteins appear to inhibit the nuclear release of nucleocapsids. Sf9 cells were transfected with AcMNPV bacmids expressing VP39-mCherry and either Vps24-GFP, Snf7-GFP, Vps60-GFP, E231Q-GFP, or the control GFP. At 24 h p.t., the transfected cells were fixed and analyzed by confocal microscopy. Scale bar, 10 μm.

Figure 11

TEM analysis of Sf9 cells transfected with AcMNPV bacmid DNAs expressing dominant-negative ESCRT-III and Vps4 proteins. Sf9 cells were transfected with

1503 AcMNPV bacmids expressing VP39-mCherry and either GFP (A), Vps24-GFP (B), Snf7-
1504 GFP (C), Vps60-GFP (D), or E231Q-GFP (E). At 72 h p.t., the transfected cells were
1505 fixed and analyzed by transmission electron microscopy. The nuclear membrane (nm),
1506 cytoplasm membrane (cm), and nucleocapsids (white arrows) are indicated. Multiple
1507 aggregated nucleocapsids localized in the space between the inner and outer nuclear
1508 membrane are indicated by closed triangles. The numbers of post-nuclear nucleocapsids
1509 were measured (F) and these include those residing in the cytoplasm, and budding
1510 through the cytoplasmic membrane. Numbers were calculated from thirteen cells for
1511 each construct. Scale bar, 1 μm. **, $p<0.0005$ (by unpaired *t* test).

1512 **Figure 12**

1513 **BiFC analysis of the interaction of ESCRT-III and AcMNPV proteins.** (A) Sf9 cells
1514 were transfected with plasmids expressing each construct consisting of the N- or C-
1515 terminal domain of mCherry (Nm and Cm) fused each ESCRT-III or viral protein. At 36 h
1516 p.t., the expression of each fusion protein construct was analyzed by Western blot
1517 analysis with anti-HA MAb (ESCRT-III proteins) or an anti-Myc polyclonal antibody (viral
1518 proteins), gels spliced for labeling purposes. (B) Fluorescence complementation in cells
1519 expressing Nm and Cm fused ESCRT-III and viral proteins. Sf9 cells were co-transfected
1520 with two plasmids separately expressing Nm or Cm fused ESCRT-III or viral proteins. At
1521 36 h p.t., the cells were photographed using epifluorescent microscopy. Labels on the
1522 left and top identify the co-transfected construct pairs in each panel. Cell boundaries
1523 were traced with circled dash lines. (C) The bar graphs show the percentages of
1524 mCherry-positive cells in co-transfected Sf9 cells expressing Nm and Cm fused ESCRT-
1525 III and viral proteins. The pairs of co-transfected constructs are indicated below the X-

axis of each graph. Error bars represent standard deviations from the mean of three replicates.

Figure 13

Co-immunoprecipitation and BiFC analysis of interactions of Vps4 and AcMNPV proteins. (A-D) Sf9 cells were transfected with the indicated (+ or -) plasmids or combinations of plasmids expressing either HA-tagged viral proteins or Myc-tagged Vps4 or modified Vps4 constructs (E231Q and K176Q). At 36 h p.t., the transfected and co-transfected cells were separately lysed and subjected to immunoprecipitation with anti-HA monoclonal antibodies and protein-G agarose. The precipitates (Co-IP) were detected on Western blots with an anti-Myc polyclonal antibody (right panel in each group). The cell lysates (Lysate) were also examined on Western blots with an anti-HA monoclonal antibody (Lysate, top panels) or an anti-Myc polyclonal antibody (Lysate, bottom panels). Abs, antibodies. (E) Sf9 cells were transfected with a plasmid expressing the N- or C-terminal domain of mCherry (Nm and Cm) fused with Vps4, Vps4 with DN mutations (E231Q and K176Q), or viral proteins (Ac11, Ac93, Ac103, or GP41,). At 36 h p.t., expression of the fusion proteins was analyzed by Western blotting using anti-HA MAb (Vps4 and its DN mutations K176Q and E231Q) or an anti-Myc polyclonal antibody (viral proteins), gels spliced for labeling purposes. (F) BiFC analysis of cells co-expressing Vps4 and viral protein pairs. Sf9 cells were co-transfected with two plasmids: one that expressed Nm-fused Vps4, E231Q, or K176Q, and a second plasmid that expressed Cm-fused viral proteins Ac11, Ac93, Ac103, or GP41. At 36 h p.t., the cells were photographed using epifluorescent microscopy. Labels on the left and top identify the co-transfected construct pairs in each panel. Cell boundaries were traced with circled

dash lines. (G) The bar graphs show the percentages of mCherry-positive cells in co-transfected Sf9 cells expressing Nm and Cm fused Vps4 and viral proteins. The pairs of co-transfected constructs are indicated below the X-axis of each graph. Error bars represent standard deviations from the mean of three replicates.

Figure 14

BiFC analysis of interactions of AcMNPV proteins. (A) Sf9 cells were transfected with plasmids expressing the N- or C-terminal domain of mCherry (Nm or Cm) fused to viral proteins (Ac11, Ac76, Ac78, Ac93, Ac103, Ac146, and GP41). At 36 h p.t., the expression of each fusion protein was analyzed by Western blotting using anti-HA MAb (Nm-fused viral proteins) or an anti-Myc polyclonal antibody (Cm-fused viral proteins) for detection, gels spliced for labeling purposes. (B) BiFC analysis of cells co-expressing Nm- and Cm-fused viral proteins. Sf9 cells were co-transfected with two plasmids, separately expressing Nm or Cm fused viral proteins. The pairs of co-transfected constructs are indicated at the top and left of each panel. At 36 h p.t., cells were photographed using epifluorescence microscopy and analyzed. Cell boundaries were traced with circled dash lines. (C) The bar graphs show the percentages of mCherry-positive cells in transfected Sf9 cells expressing Nm and Cm fused viral proteins. The pairs of co-transfected constructs are indicated below the X-axis of each graph. Error bars represent standard deviations from the mean of three replicates.

Figure 15

Schematic representation of protein-protein interaction network of ESCRT-III proteins and Vps4, and viral proteins and ESCRT-III/Vps4. ESCRT-III components and viral proteins that interact with themselves are shown as shaded circles. The top left

1572 panel shows interactions among ESCRT-III proteins (Vps2B, Vps20, Vps24, Vps46,
1573 Vps60, and Snf7) and Vps4. The panel on the right shows interactions among the viral
1574 proteins (inner circle, Ac11, Ac76, Ac78, Ac93, Ac103, Ac142, Ac146, and GP41) and
1575 interactions between each viral protein (inner group) and ESCRT-III proteins (outer
1576 group, Vps2B, Vps20, Vps24, Vps46, Vps60, and Snf7). The lower left panel shows
1577 interactions between cellular Vps4 and viral proteins (Ac93, Ac103, and GP41).

1578 **Figure 16**

1579 **A hypothetical model of the interaction of the viral proteins and ESCRT-III/Vps4**
1580 **in nuclear egress of progeny nucleocapsids**. (A) In AcMNPV infected cells, the
1581 nuclear membrane associated Ac76 may initiate the nuclear membrane protrusion. Ac76
1582 interacts with Ac93 and Ac78 which may form a complex that interacts with Ac103, that
1583 in turn interacts with nucleocapsid-associated protein Ac146, to target the progeny
1584 nucleocapsids to the budding region on the nuclear membrane. (B) A viral protein
1585 complex (Ac76, Ac93, Ac78 and possibly Ac142) may recruit the core components of
1586 ESCRT-III to the budding region and result in formation of the Snf7 filament that
1587 constricts the nuclear membrane, releasing a double-membraned vesicle containing
1588 nucleocapsids. (C) After pinching off of the double-membraned vesicle, the viral protein
1589 complex within the nucleus recruits Vps4 and its regulatory ESCRT-III proteins (Vps46
1590 and Vps60) to form the activated Vps4 complex, which disassembles and recycles the
1591 ESCRT-III complex. BV, budded virions; CCV, clathrin-coated vesicle; DN, dominant
1592 negative; EE, early endosome; ER, endoplasmic reticulum; INM, inner nuclear
1593 membrane; LE/MVBs, late endosome/multivesicular bodies; NPC, nuclear pore complex;
1594 ONM, outer nuclear membrane; VS, virogenic stroma.

Figure 1

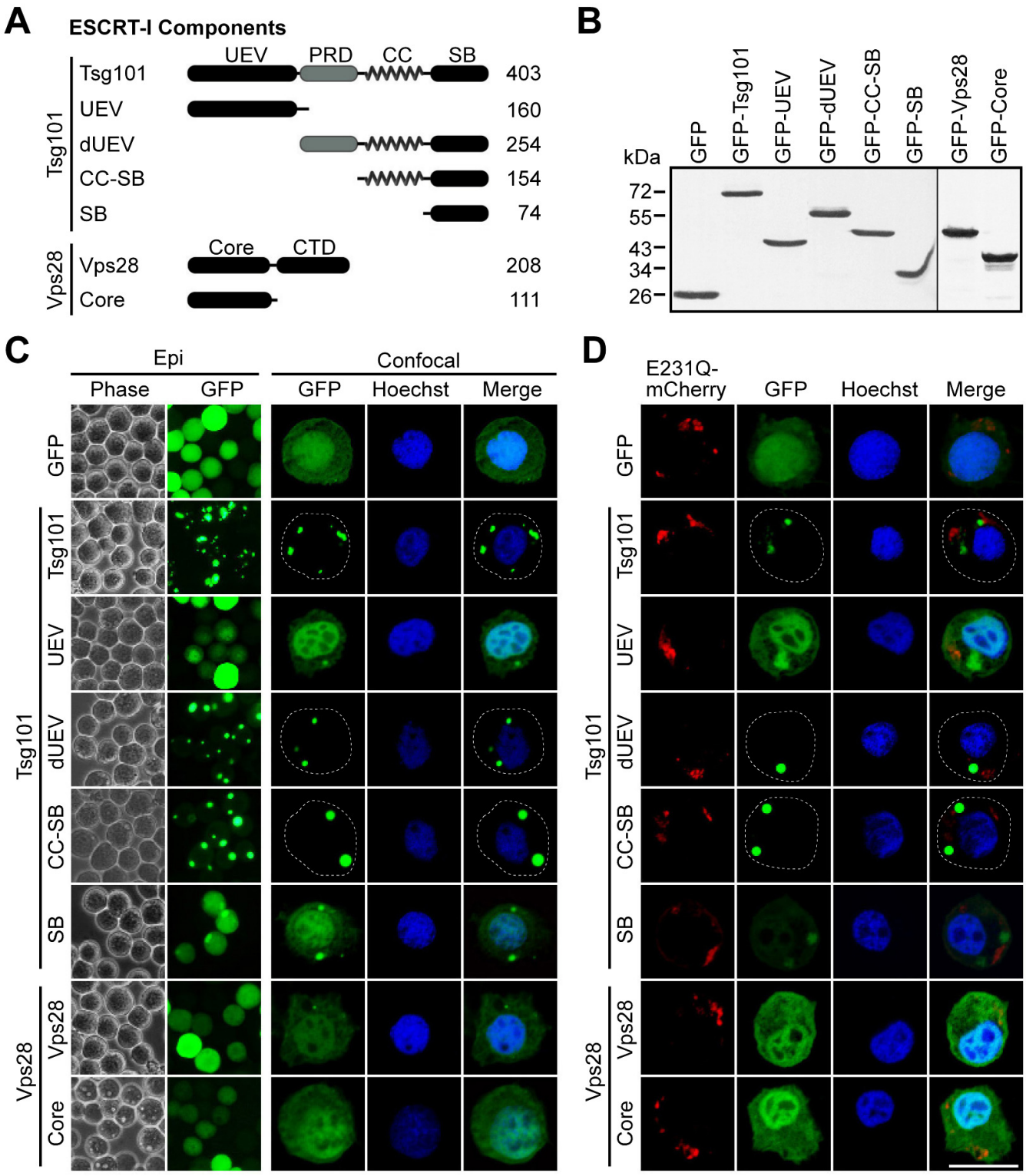

Figure 2

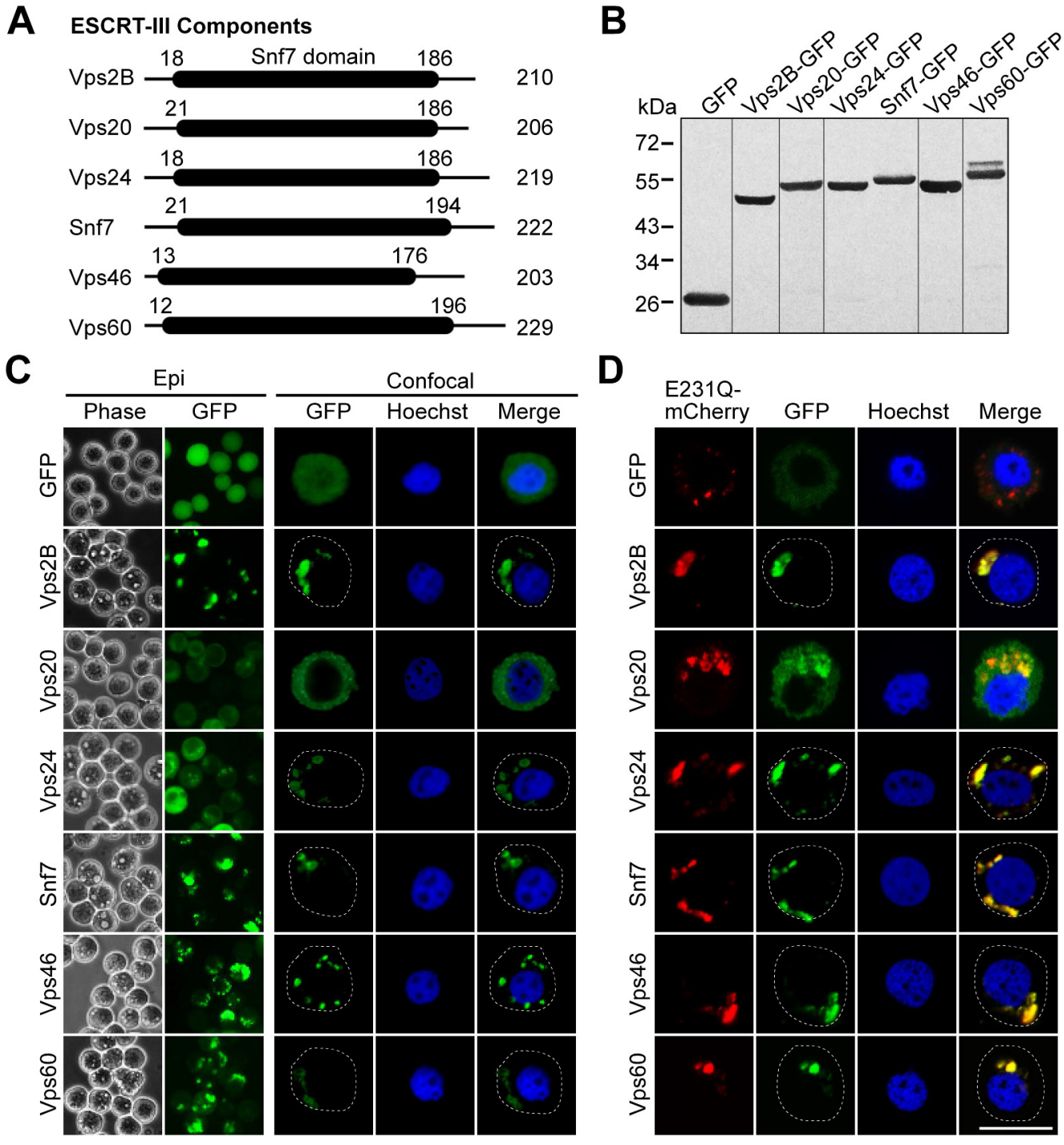

Figure 3

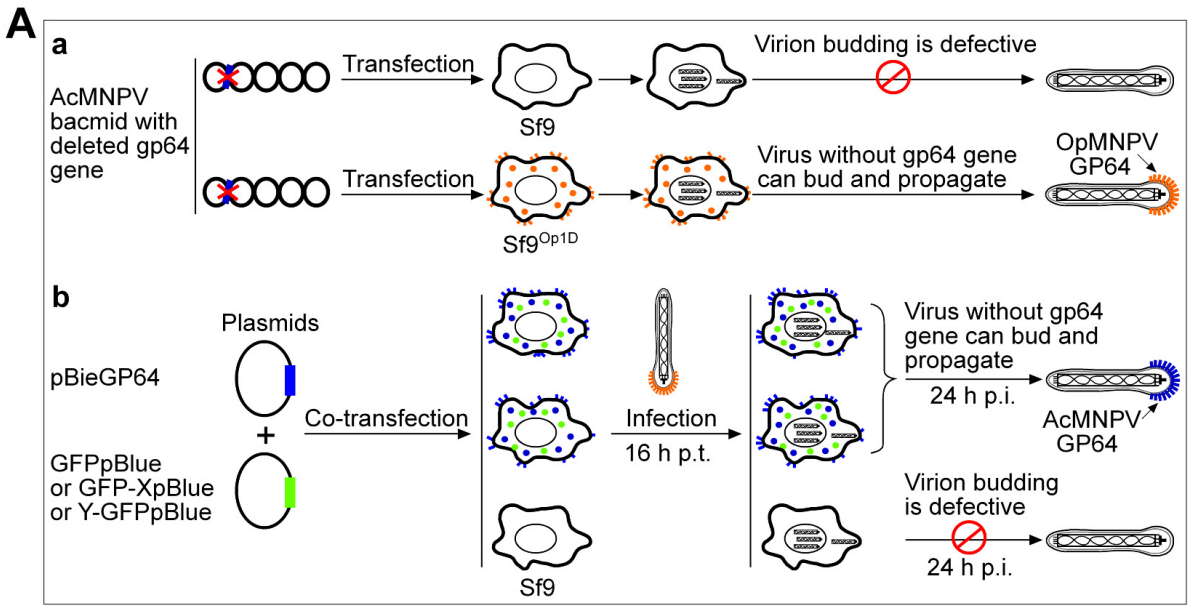

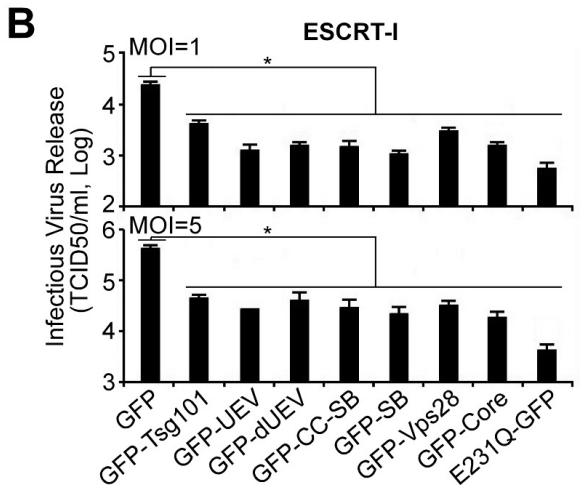

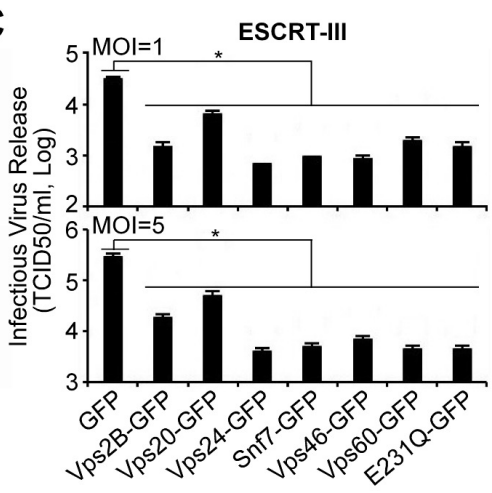

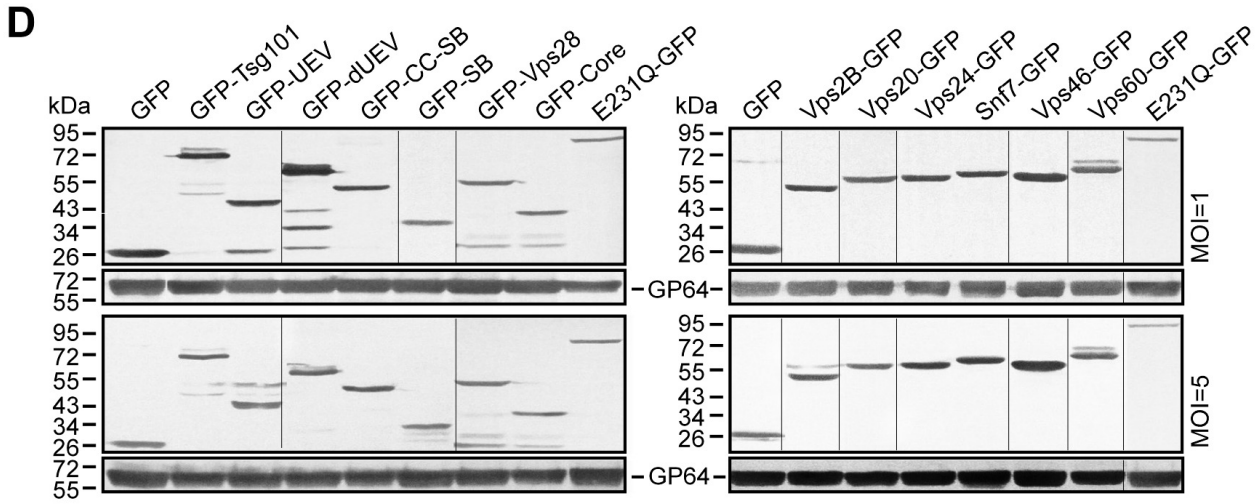

Figure 4

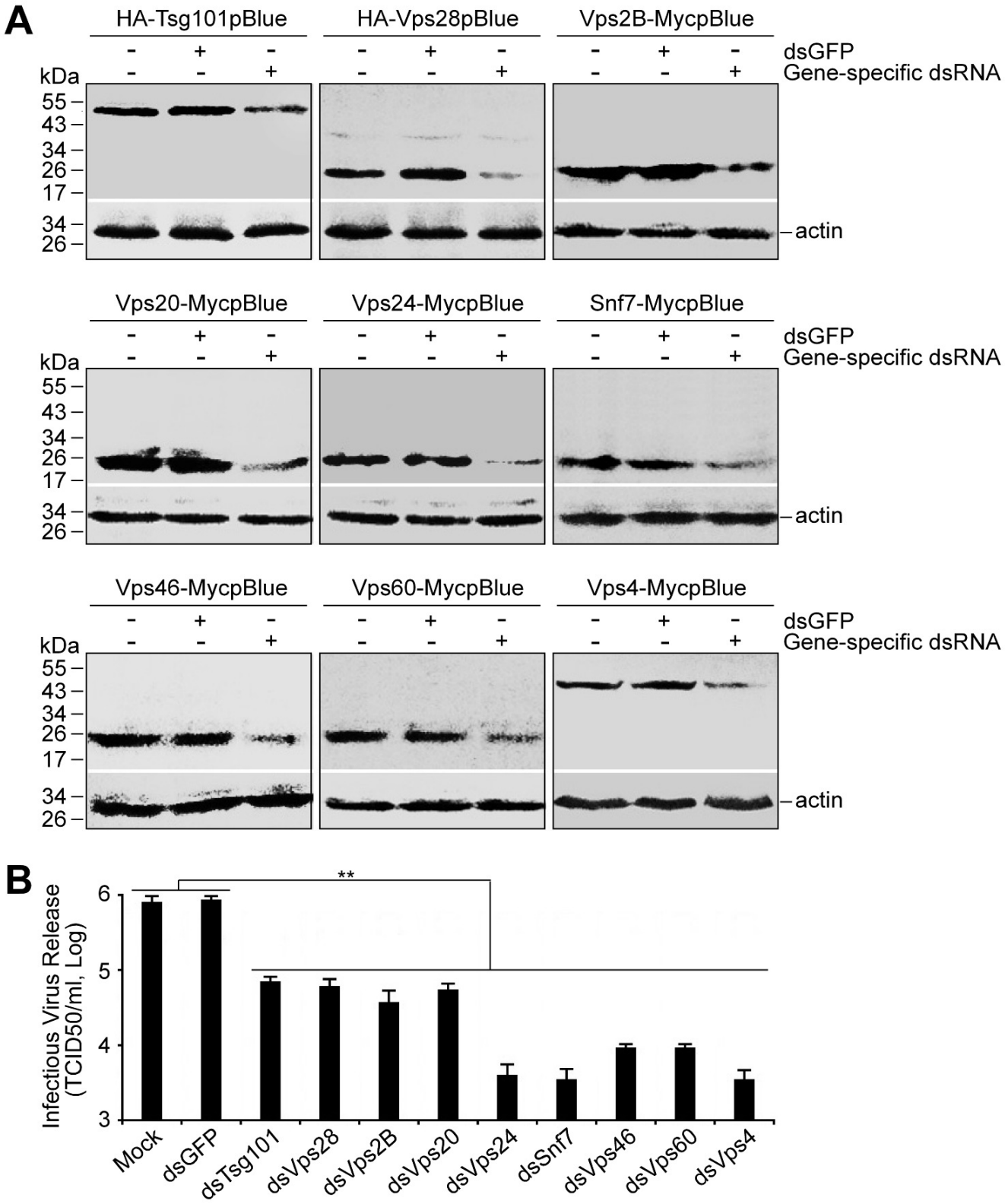

Figure 5

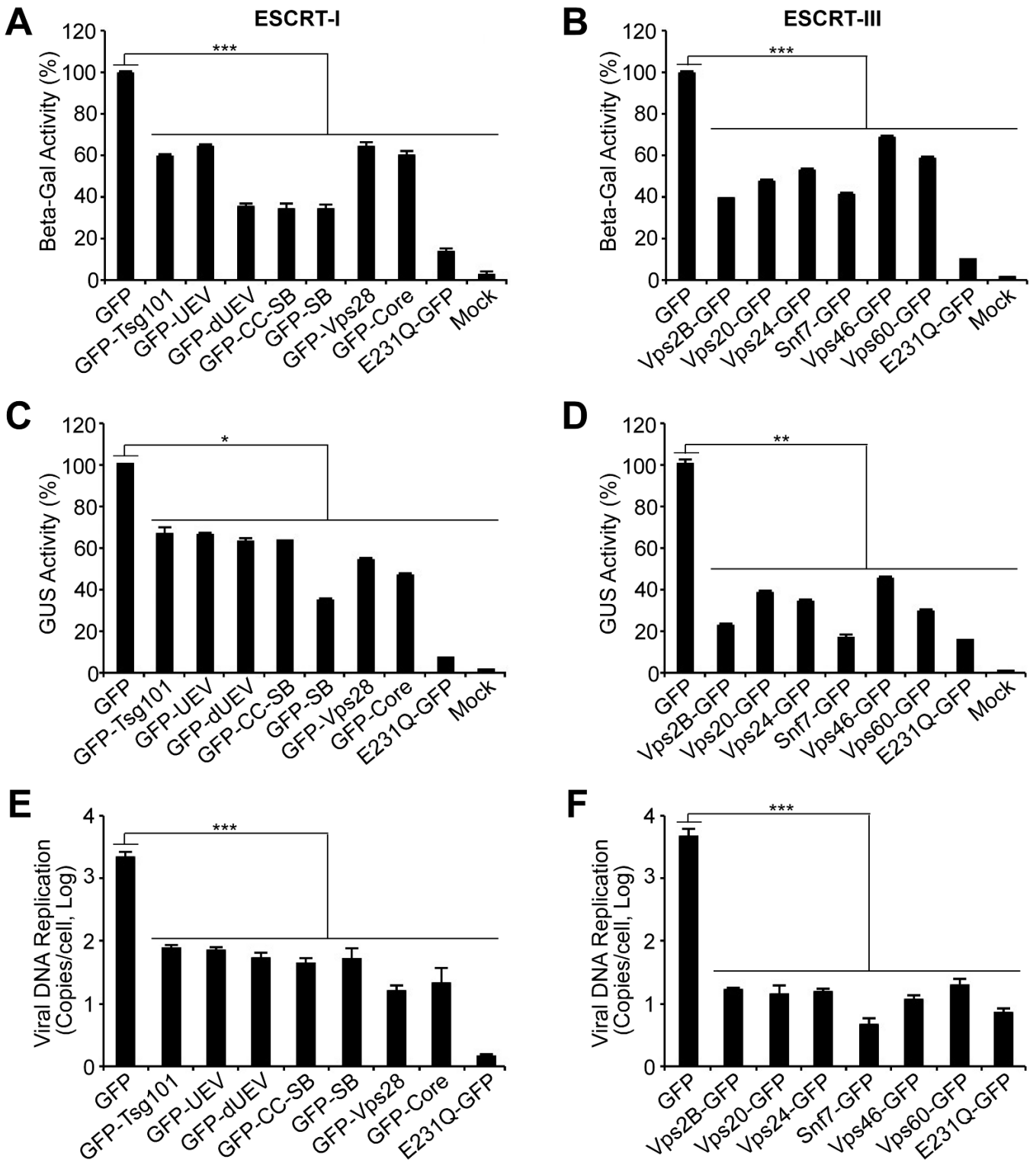

Figure 6

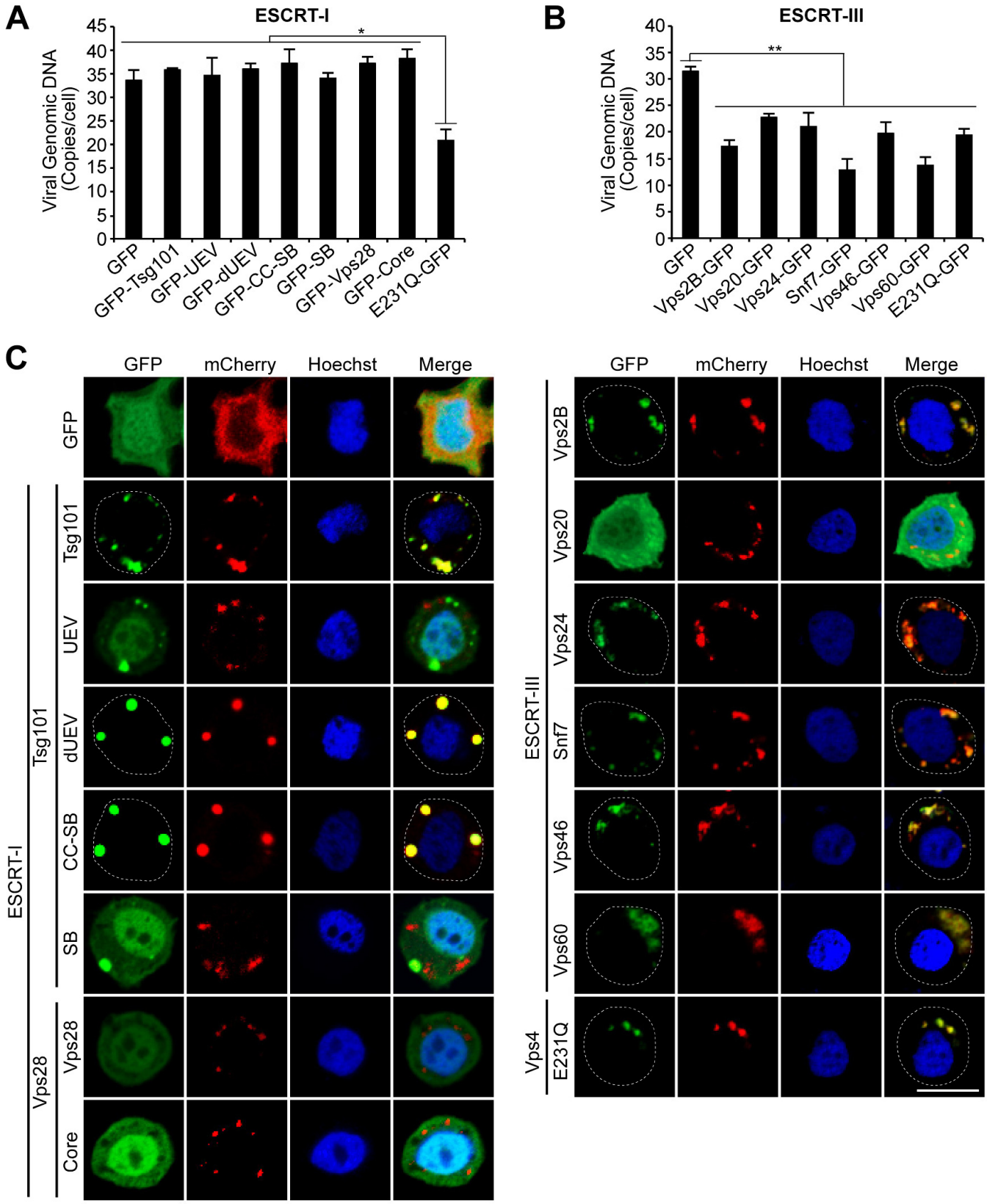

Figure 7

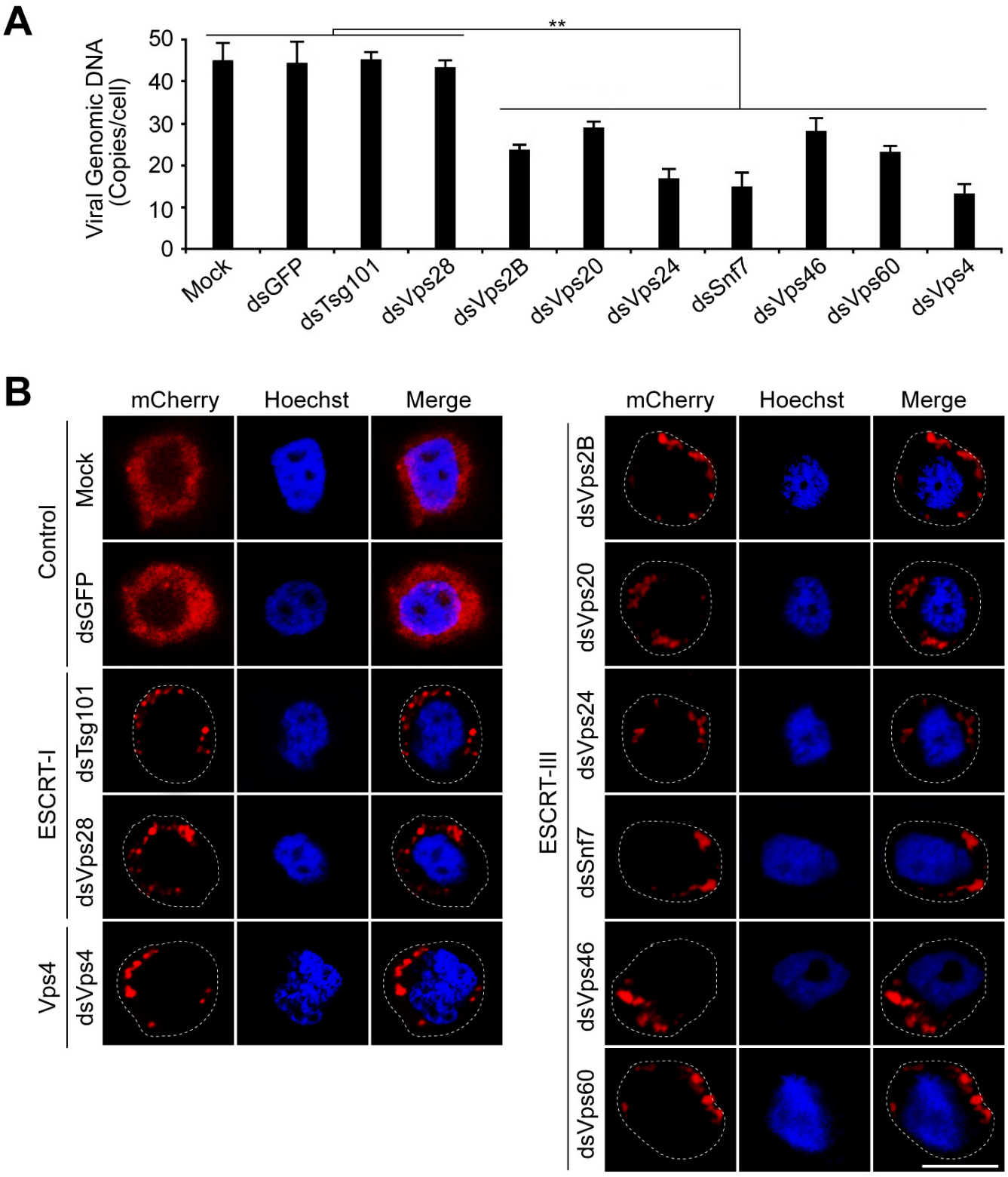

Figure 8

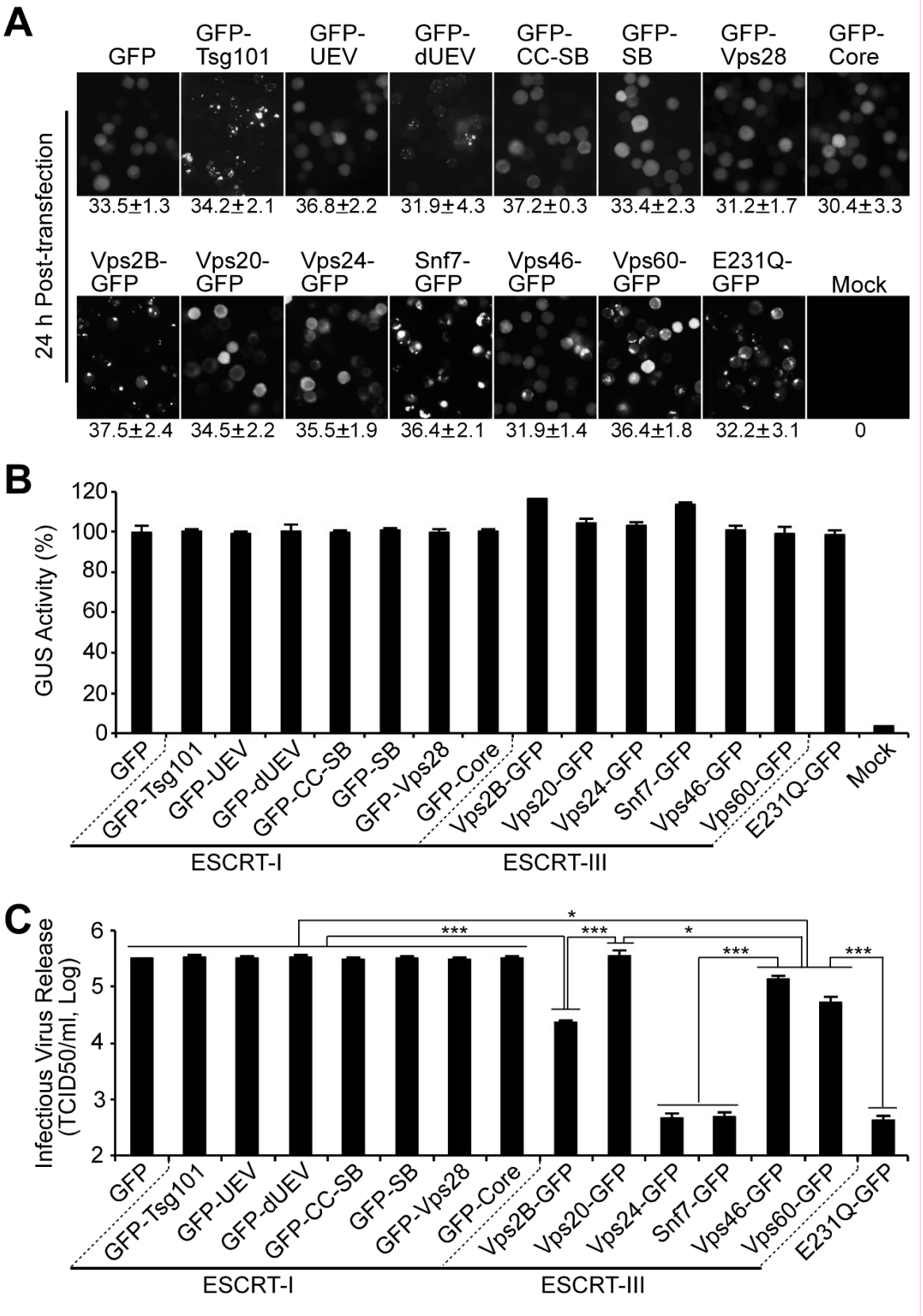

Figure 9

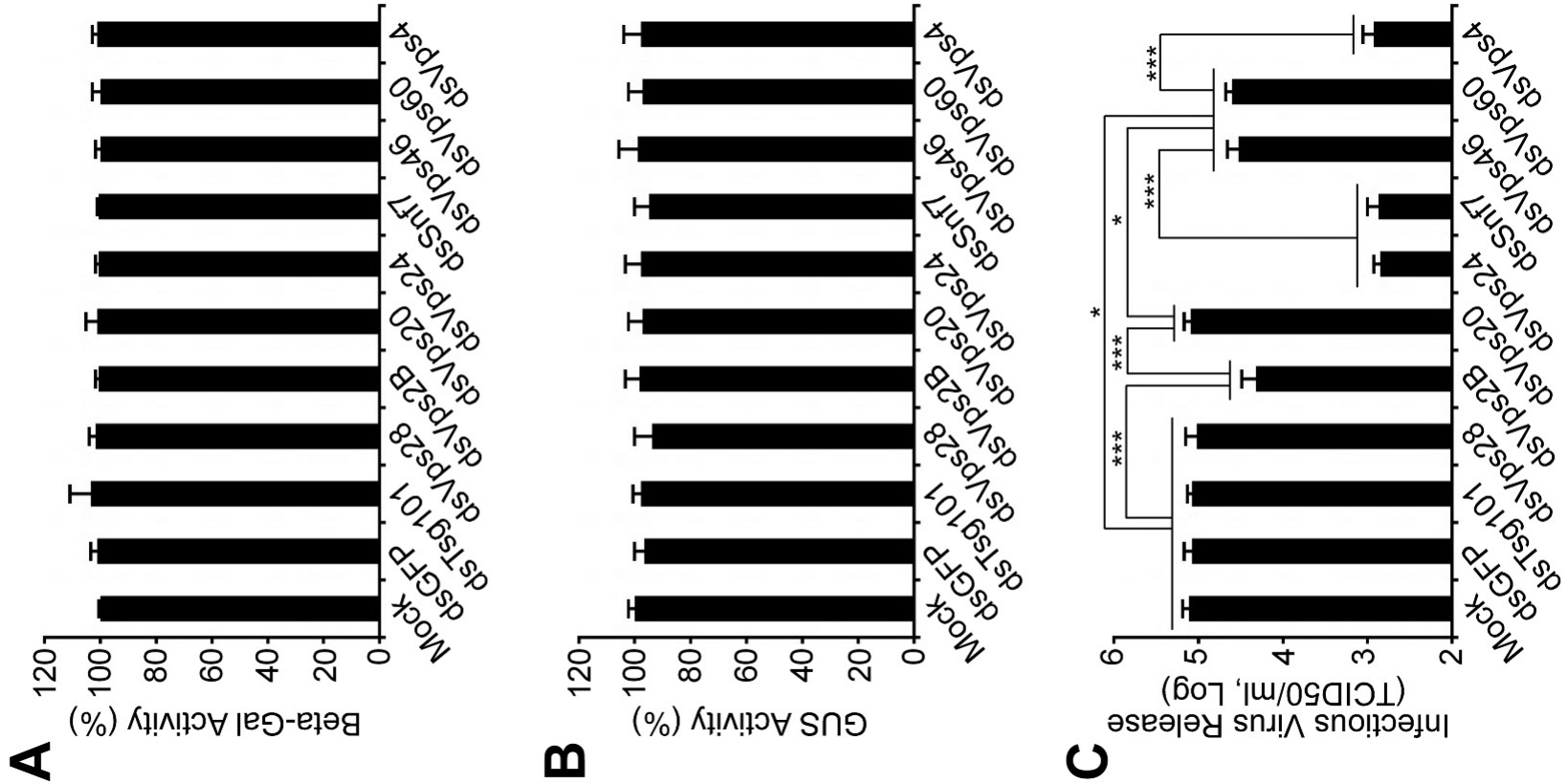

Figure 10

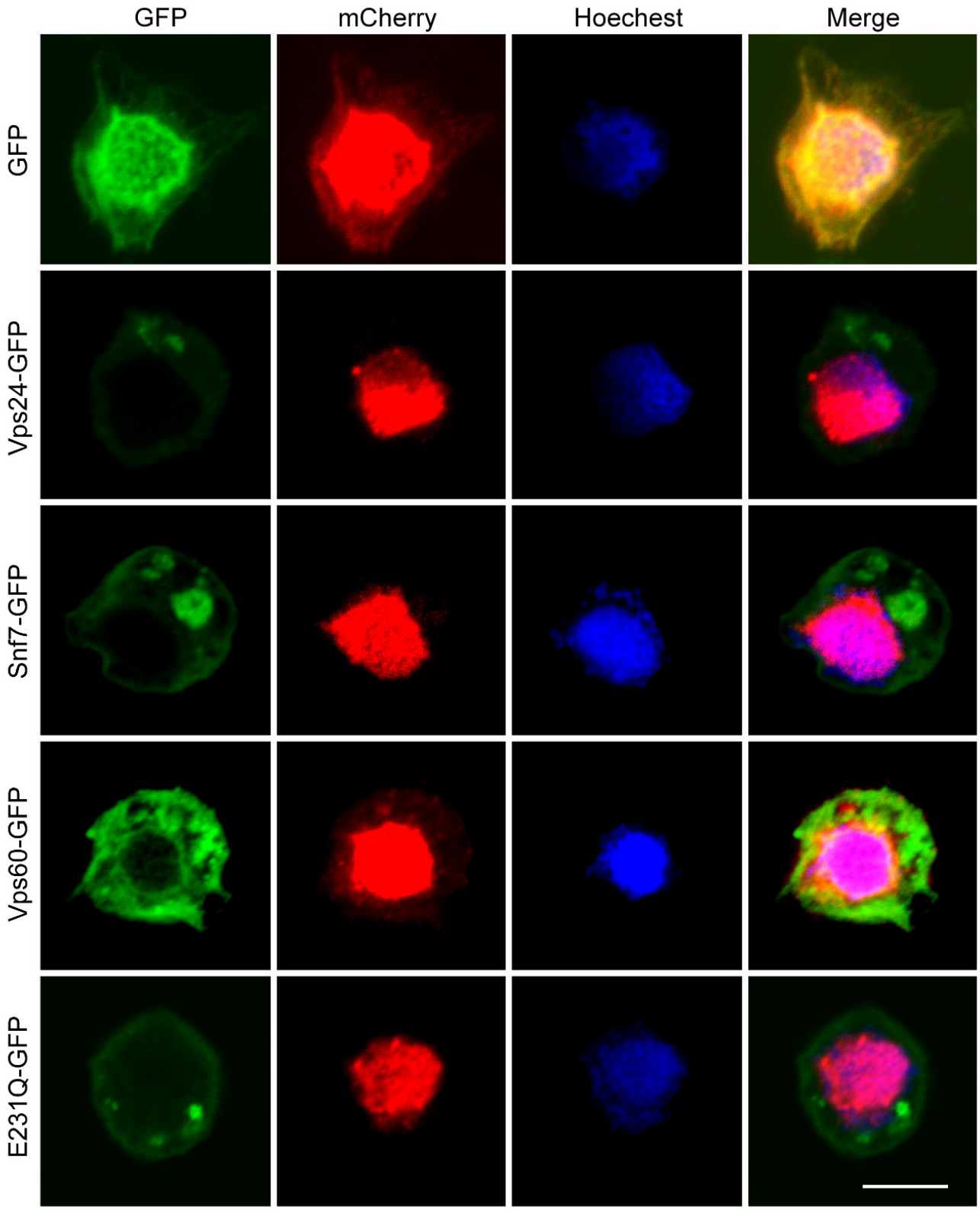

Figure 11

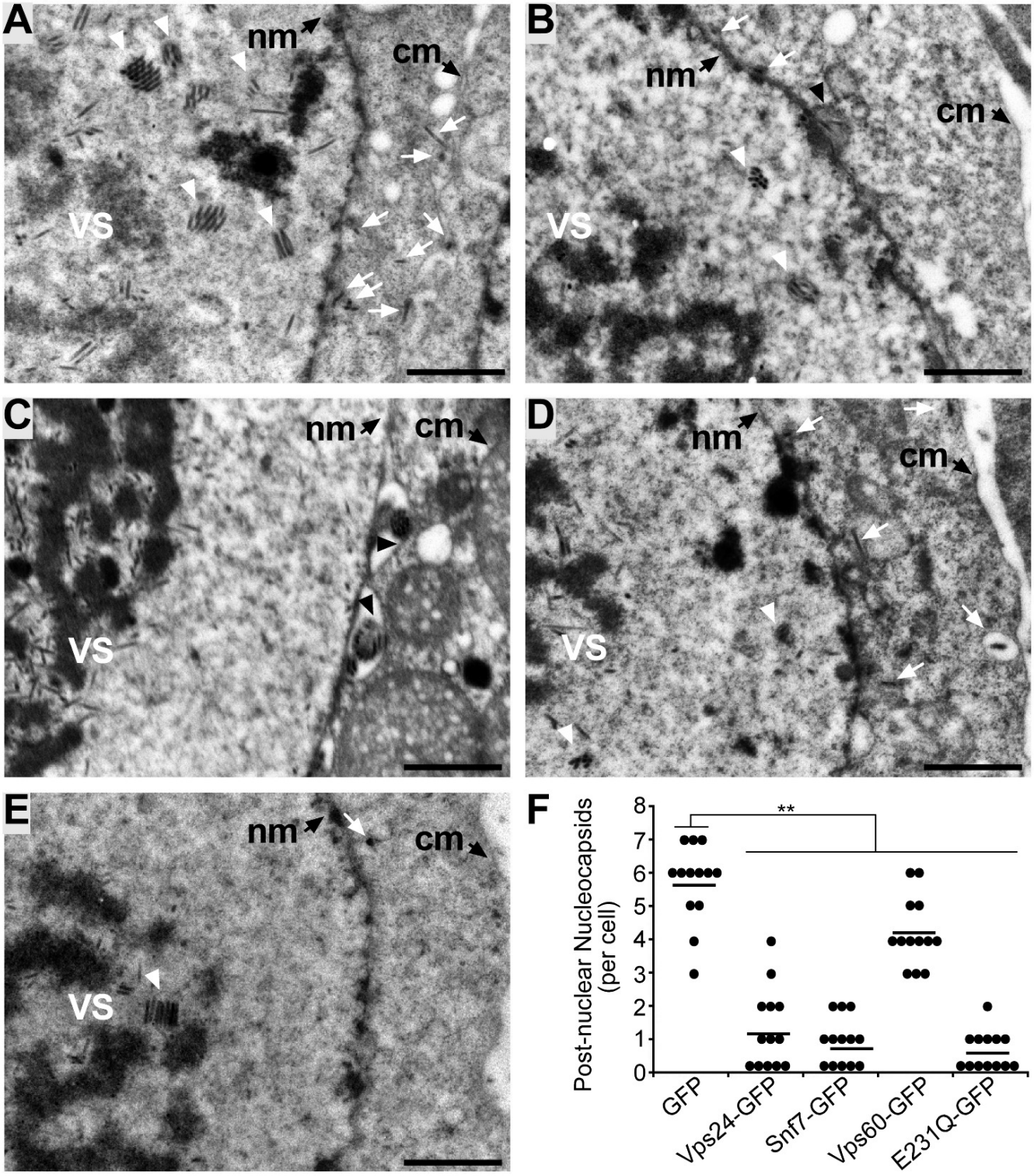

Figure 12

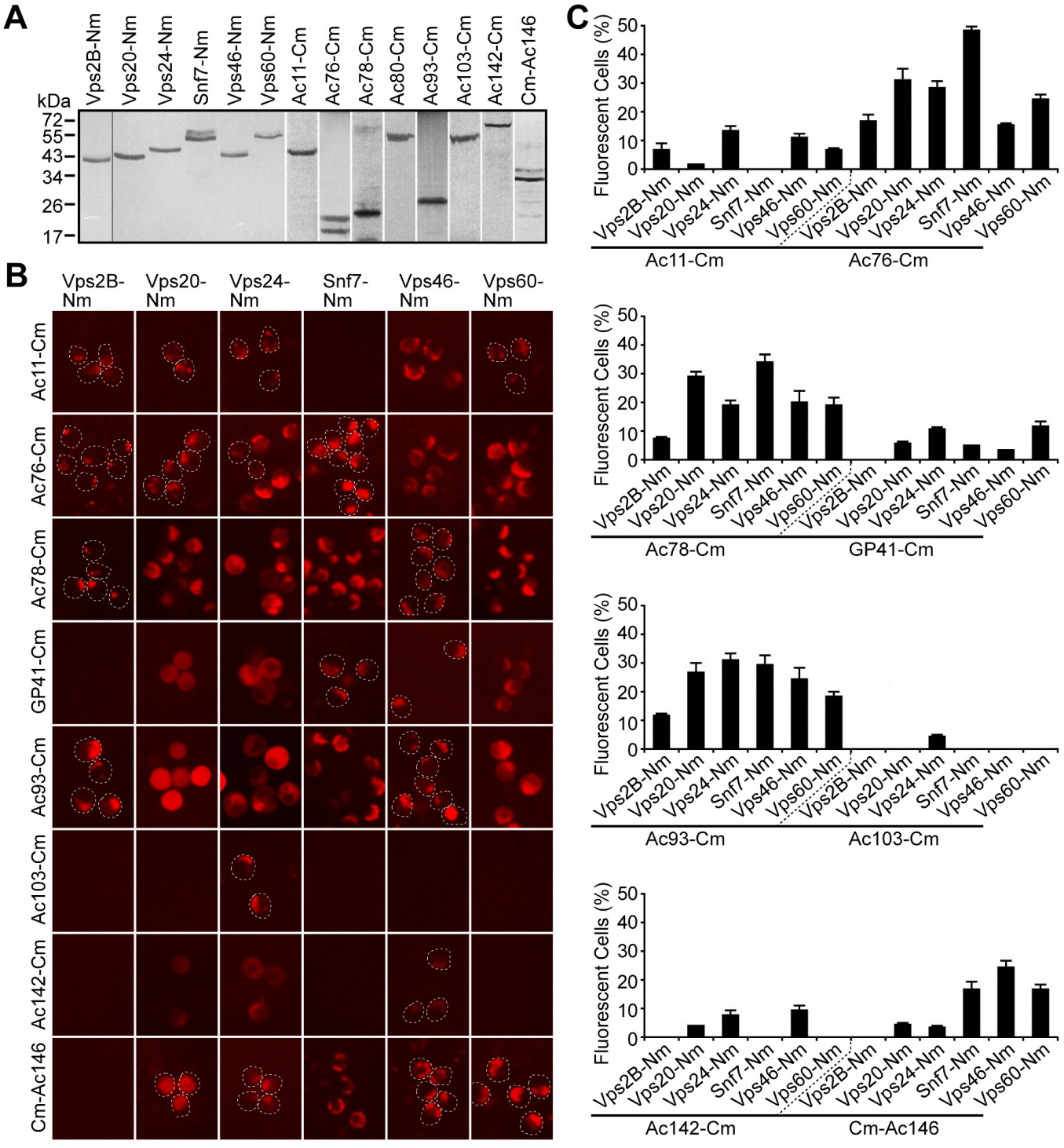

Figure 13

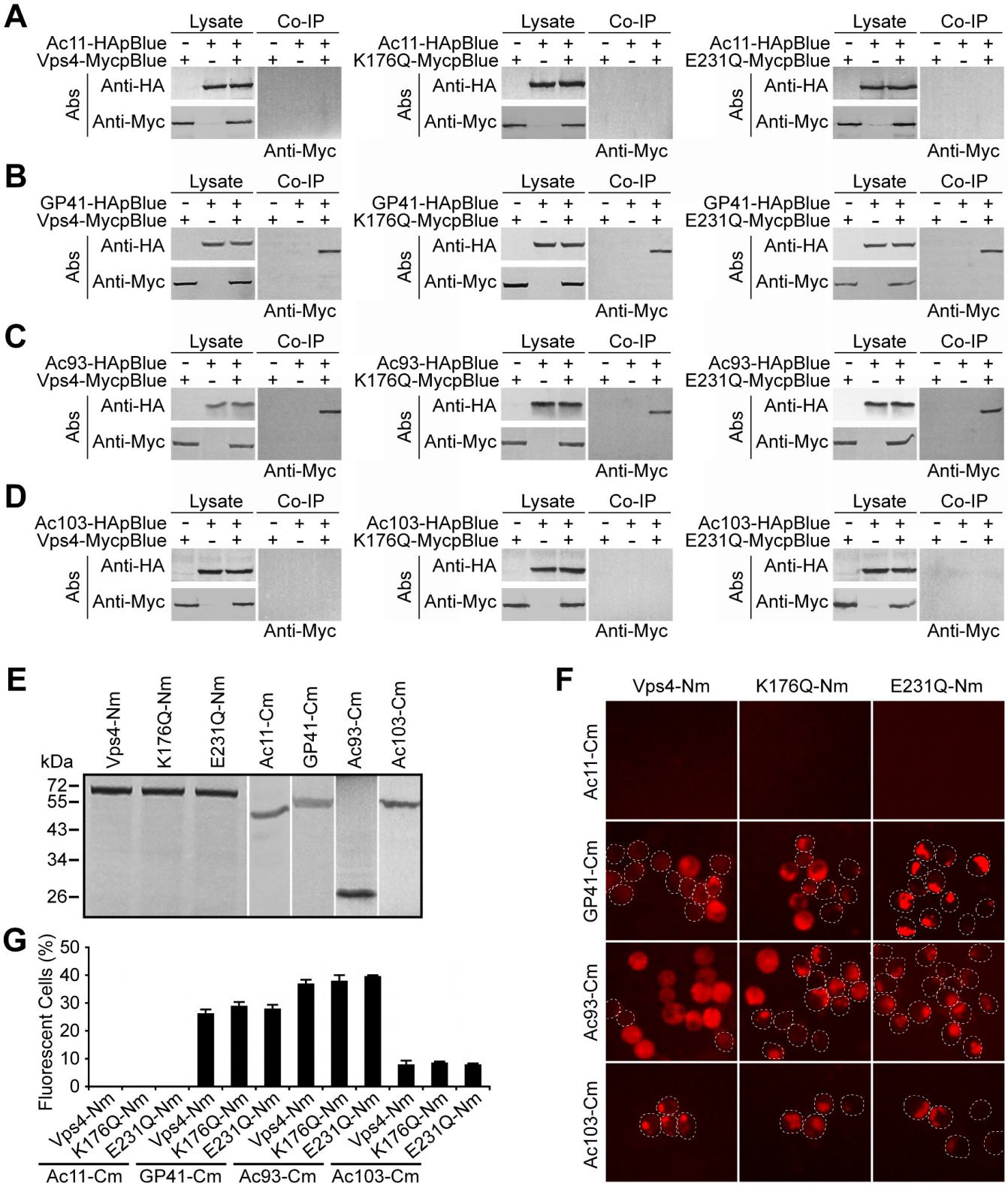

Figure 14

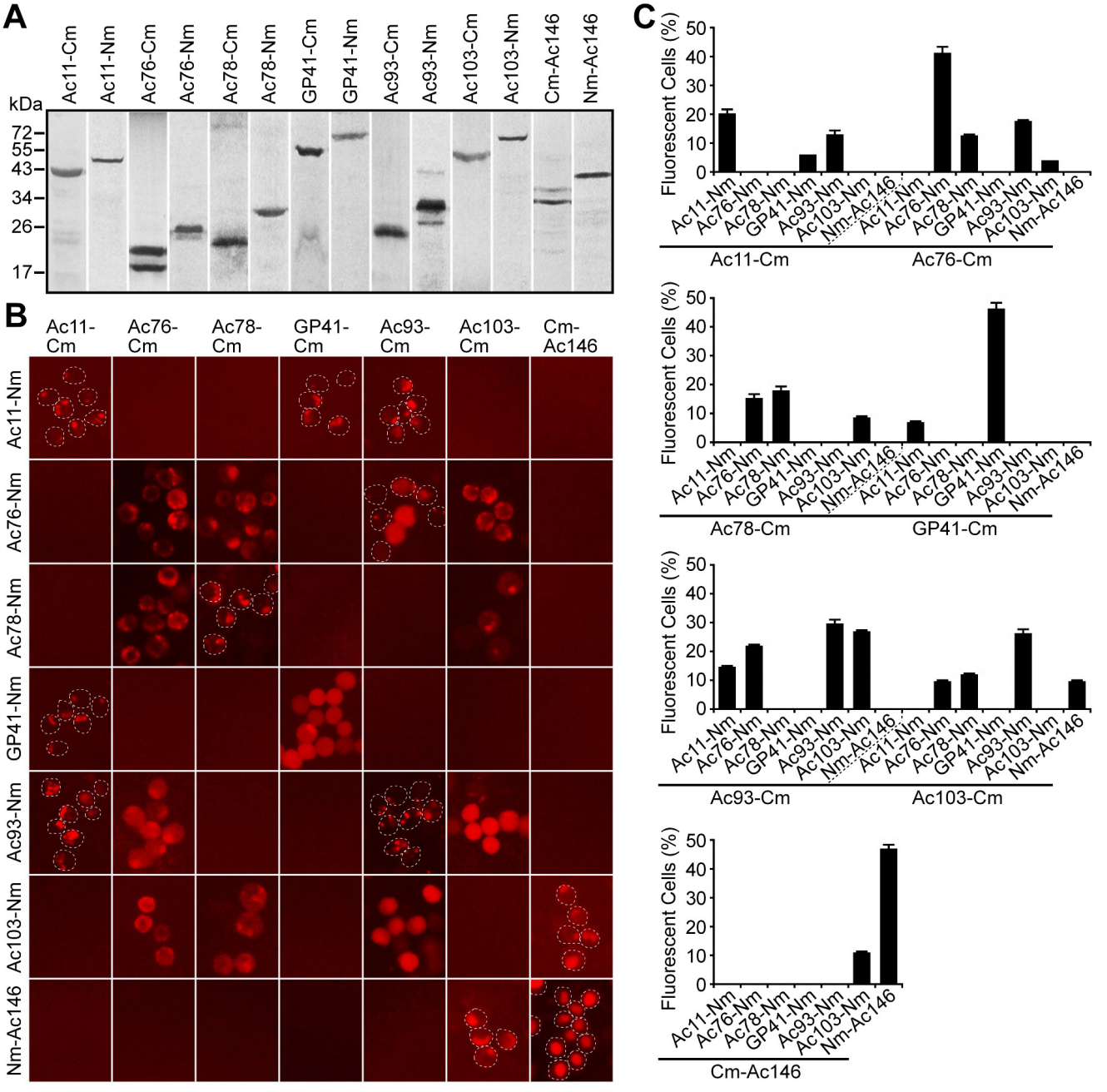

Figure 15

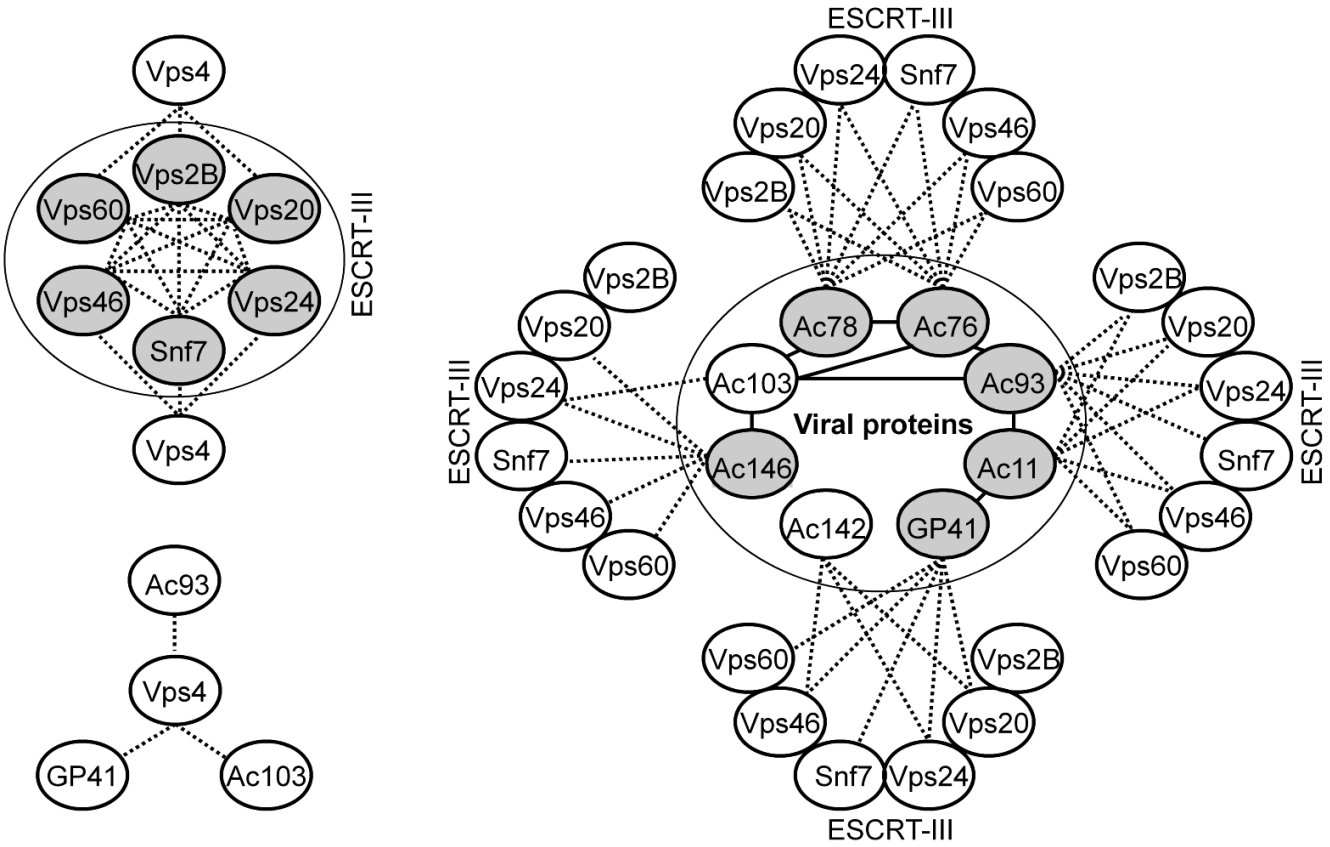

Figure 16

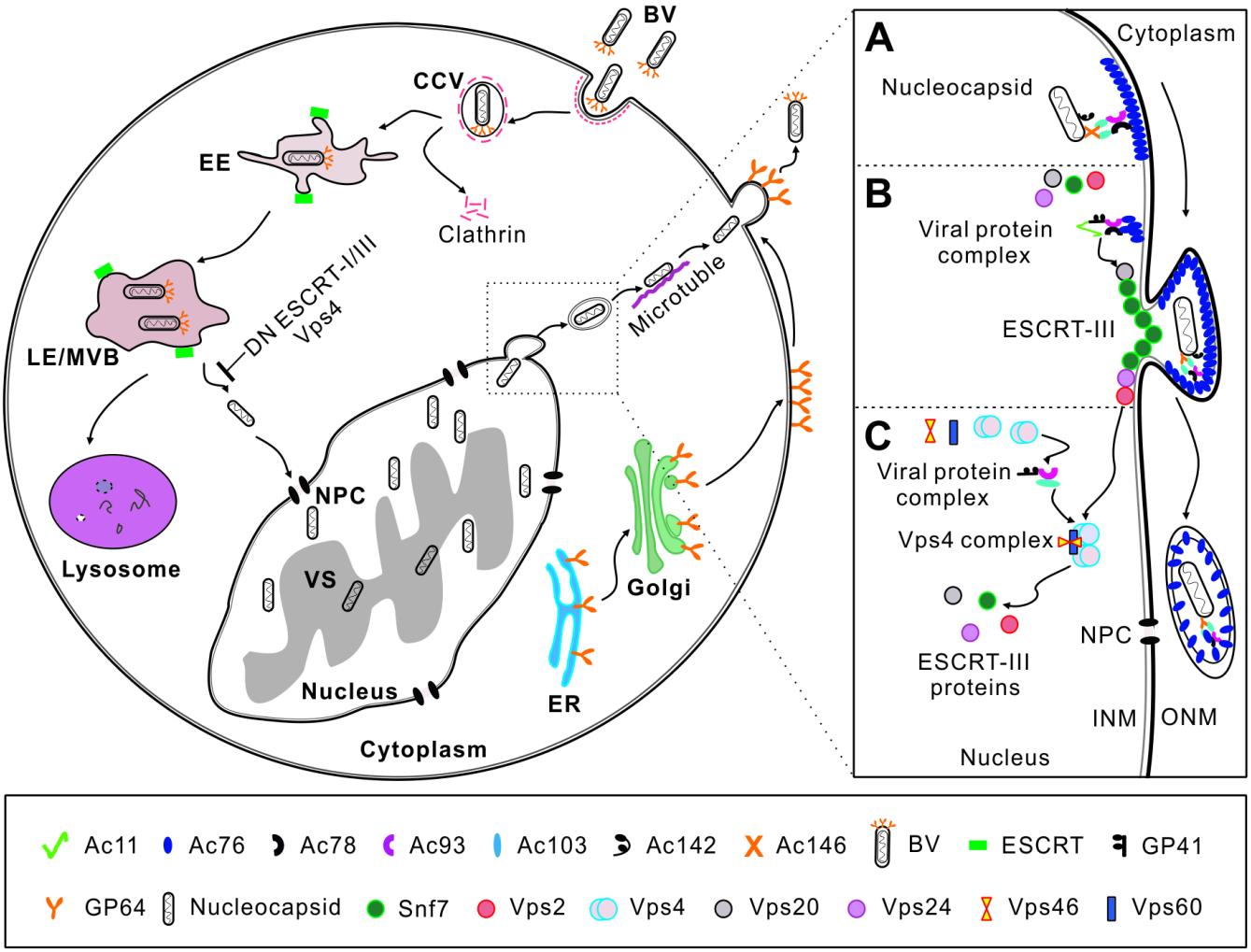

Table 1. PCR primers

Primer name	Sequence (5' to 3')	Purpose
Ac11XF	atatctagaatgtctctcgctgcaaagttaat	Amplification of the ORF of AcMNPV genes *ac11*, *ac76*, *ac78*, *ac80* (*gp41*), *ac93*, *ac103*, *ac142*, *ac146* and *lef-3*
Ac11ER	atagaattcttgtaaatgtttattatttaaaaacg	
Ac76XF	aattctagaatgaatttatatttgttgttg	
Ac76ER	aatgaattcatctattgagctggtatttttgt	
Ac78XF	atatctagaatgaatttggacgtgccct	
Ac78ER	atagaattcatcaaatttattaaaaacaaaagga	
Ac80XF	ataatctagaatgacagatgaacgtggca	
Ac80ER	ataagaattctgcactgcgccctttcgtgtt	
Ac93XF	aattctagaatggcgactagcaaaacgat	
Ac93ER	aatgaattcatttacaatttcaattccaatg	
Ac103XF	aattctagaatgtgcgcttacagattacaatac	
Ac103ER	aatgaattctttattgaagcaatcatggttgag	
Ac142XF	aattctagaatgagtggtggcggcaacttgt	
Ac142ER	aatgaattcttgtaccgagtcggggattaataa	
Ac146BF	aatggatccatgaacgtcaatttatactgc	
Ac146ER	aatgaattcctatgaagagcgggtttc	
Lef3XF	atatctagaatggcgaccaaaagatctttg	
Lef3ER	attgaattccaaaaatttatattcattttc	
Tsg101F	gggatgtgattctgtgattt	Amplification of the ORF of ESCRT-I components Tsg101 and Vps28 and their truncated forms
Tsg101R	acatcatccgagtatgactca	
Tsg101BF	ataggatccatggctaacgacgatgtagtg	
Tsg101ER	atagaattcttagcacgccaactgagccttct	
UEVER	ataagaattctggcatgaaagagtttactgggt	
dUEVXF	aagtaatctagaatgagagcgccttacccagtaaact	
CC-SBXF	ataatctagaatggtagaagataaactacgaaggag	
SBXF	ataatctagaatggacgaagctgttgtgaccactg	
Vps28F	aaccttagccttgccttaacaat	
Vps28R	ttgagctggtcacatcgatgac	
Vps28BF	aatggatccatgcaggacacaagaccagaa	
Vps28ER	atagaattctcagtccttgtgcaggaacttg	
CoreER	attgaattctcagcccttgtcgtccttgatgaggt	
Vps2BF	atcgggaagtggtagttata	Amplification of the ORF of the ESCRT-III components Vps2B, Vps20, Vps24, Snf7, Vps46, and Vps60
Vps2BR	agagattatatttcatgtgcgcg	
Vps2BXF	aattctagaatggatttcttctttggcaagca	
Vps2BER	aatgaattcggactttagcttagctaattg	
Vps20F	tatgtagataaggctacaacat	
Vps20R	tatactttaaagcctatataca	
Vps20XF	aattctagaatgggttccttattcggtaaac	
Vps20ER	aatgaattcagcttcggctgctaatttga	
Vps24SP1	agagttgctgggtcattgcaga	
Vps24SP2	tggcatcattgaggagatgct	
Vps24F	aataggtaattgttatattataac	
Vps24R	gcaatagtcaatccgtggcggct	
Vps24XF	aattctagaatgggcctgtttggtaaatcacc	
Vps24ER	aatgaattccgaagacctgagtgcctctaacc	
Snf7F	tctcttgcaatacgttgttt	
Snf7R	accagtatacatcgacgtgctgtg	
Snf7mF	acaagagtttctggagaagaaaatcgat	
Snf7mR	atcgattttcttctccagaaactcttgt	
Snf7XF	atatctagaatgagttttctggggaagttatt	
Snf7ER	atagaattctgtggcccaagactgcaactgtg	
Vps46F	accctgtgcttagtgctaagctt	
Vps46R	acatgcatcatttaggtcttaca	
Vps46XF	aattctagaatgtcttcatccgctatggaa	
Vps46ER	atagaattcttcggcttgtcgtaatcgagc	
Vps60F	tcacgatccggggcaatgaggat	
Vps60R	gtttcccagtcacgatct	
Vps60XF	aattctagaatgaacagaatattcggaag	
Vps60ER	aatctgcagcgacgatctaccgcgggaagt	
VP39pF	aatgagctcggtaccttgttcgccatcgtggaatca	Amplification of the promoter and ORF of AcMNPV *vp39*
VP39pR	aattctagaattgttgccgttataaatatg	
VP39XF	aattctagaatggcgctagtgcccgtgggt	

VP39ER	aatgaattcgacggctattcctccacctg	
GFPiF	taatacgactcactatagggacgtaaacggccacaagttc	Amplification of the double-strand (ds)DNA of GFP, the components of ESCRT-I (Tsg101, Vps28) and ESCRT-III (Vps2B, Vps20, Vps24, Snf7, Vps46, Vps60), and Vps4
GFPiR	taatacgactcactatagggtgttctgctggtagtggtcg	
Tsg101iF	taatacgactcactatagggagtggacacagaatggctcc	
Tsg101iR	taatacgactcactatagggttccttcagcctccttcgta	
Vps28iF	taatacgactcactatagggagcatgacaacatggcagag	
Vps28iR	taatacgactcactataggggcttgtccacccactcttgt	
Vps2BiF	taatacgactcactatagggacgatgggagcaaacatagc	
Vps2BiR	taatacgactcactatagggccgcatctttggttgattct	
Vps20iF	taatacgactcactatagggcctgcaagcagagtgactga	
Vps20iR	taatacgactcactatagggttggtcacccacatcaagaa	
Vps24iF	taatacgactcactatagggaagctgcagccaagaatgat	
Vps24iR	taatacgactcactatagggcatgcctgacatggtctcat	
Snf7iF	taatacgactcactatagggtctggggaagttattcggtg	
Snf7iR	taatacgactcactatagggtatgagccaatttcatggca	
Vps46iF	taatacgactcactataggggcacggatacatgcagagaa	
Vps46iR	taatacgactcactatagggaaccagcctcatcagcaact	
Vps60iF	taatacgactcactatagggtattcggaaggggaaaacct	
Vps60iR	taatacgactcactatagggctgtgtgactccgtccttca	
Vps4iF	taatacgactcactatagggggaaacacgaggcatcaact	
Vps4iR	taatacgactcactatagggaacttcctaagccggaccat	
nGFPF	Aattctagaatggtgagcaagggcgaggag	Construction of pIEnGFP and pIEcGFP
GFPR	aatggatcccttgtacagctcgtccatgcc	
cGFPF	aatgaattcatggtgagcaagggcgaggag	
GFPpAF	catggacgagctgtacaagtaaatgtaataataaaaattgtatca	
GFPpAR	tgatacaatttttattattacatttacttgtacagctcgtccatg	
64pAR	attaagcttcacactcgctatttggaacat	

Table 2. Plasmids constructed in this study

Purpose	Construct name
Expression of ESCRT-I and ESCRT-III proteins	GFP-Tsg101pBlue, GFP-UEVpBlue, GFP-dUEVpBlue, GFP-CC-SBpBlue, GFP-SBpBlue, GFP-Vps28pBlue, GFP-CorepBlue, HA-Tsg101pBlue, HA-Vps28pBlue, Vps2B-GFPpBlue, Vps20-GFPpBlue, Vps24-GFPpBlue, Snf7-GFPpBlue, Vps46-GFPpBlue, Vps60-GFPpBlue
Co-immunoprecipitation	Ac11-HApBlue, Ac76-HApBlue, Ac78-HApBlue, GP41-HApBlue, Ac93-HApBlue, Ac103-HApBlue, Ac142-HApBlue, HA-Ac146pBlue, Ac11-MycpBlue, Ac76-MycpBlue, Ac78-MycpBlue, GP41-MycpBlue, Ac93-MycpBlue, Ac103-MycpBlue, Ac142-MycpBlue, Myc-Ac146pBlue, Lef3-MycpBlue, Vps2B-MycpBlue, Vps20-MycpBlue, Vps24-MycpBlue, Snf7-MycpBlue, Vps46-MycpBlue, Vps60-MycpBlue, Vps4-MycpBlue, K176Q-MycpBlue, E231Q-MycpBlue
Bimolecular fluorescence complementation (BiFC) assay	Ac11-CmpBlue, Ac76-CmpBlue, Ac78-CmpBlue, GP41-CmpBlue, Ac93-CmpBlue, Ac103-CmpBlue, Ac142-CmpBlue, Cm-Ac146pBlue, Lef3-CmpBlue, Ac11-NmpBlue, Ac76-NmpBlue, Ac78-NmpBlue, GP41-NmpBlue, Ac93-NmpBlue, Ac103-NmpBlue, Ac142-NmpBlue, Nm-Ac146pBlue, Vps2B-CmpBlue, Vps20-CmpBlue, Vps24-CmpBlue, Snf7-CmpBlue, Vps46-CmpBlue, Vps60-CmpBlue, Vps4-CmpBlue, K176Q-CmpBlue, E231Q-CmpBlue, Vps2B-NmpBlue, Vps20-NmpBlue, Vps24-NmpBlue, Snf7-NmpBlue, Vps46-NmpBlue, Vps60-NmpBlue, Vps4-NmpBlue, K176Q-NmpBlue, E231Q-NmpBlue

Note: Nm and Cm represent the N- and C-terminus of mCherry, respectively.

Table 3. Co-IP analysis of interactions of ESCRT-III/Vps4 and AcMNPV proteins*

AcMNPV	ESCRT-III						Vps4		
proteins	Vps2B	Vps20	Vps24	Snf7	Vps46	Vps60	Vps4	K176Q	E231Q
Ac11	+	-	+	-	+	+	-	-	-
Ac76	+	+	+	+	+	+	-	-	-
Ac78	-	+	+	+	+	+	-	-	-
GP41	-	+	+	+	+	+	+	+	+
Ac93	+	+	+	+	+	+	+	+	+
Ac103	-	-	+	-	-	-	-	-	-
Ac142	-	-	+	-	+	-	-	-	-
Ac146	-	-	+	+	+	+	-	-	-

*AcMNPV proteins were tagged with an HA epitope. ESCRT-III and Vps4 proteins were tagged with a c-Myc epitope. "+" and "-" represent positive and negative Co-IP (co-immunoprecipitation) signal, respectively. The original Co-IP data for the interaction of Vps4 and viral proteins is shown in Fig. 13, and the Co-IP data for the interaction of ESCRT-III and viral proteins is not shown.

Table 4. Co-IP analysis of interactions of AcMNPV proteins*

	Ac11	Ac76	Ac78	GP41	Ac93	Ac103	Ac142	Ac146
Ac11	+	-	-	+	+	-	-	-
Ac76	-	+	+	-	+	+	-	-
Ac78	-	+	+	-	-	+	-	-
GP41	+	-	-	+	-	-	-	-
Ac93	+	+	-	-	+	+	-	-
Ac103	-	+	+	-	+	-	-	+
Ac142	-	-	-	-	-	-	-	-
Ac146	-	-	-	-	-	+	-	+

*AcMNPV proteins were tagged with an HA and a c-Myc epitopes. "+" and "-" represent positive and negative Co-IP (co-immunoprecipitation) signal, respectively. The original Co-IP data is not shown.